Designing Advanced Ceramic Waste Forms for Electrochemical Processing Salt Waste

Fuel Cycle Research & Development

Prepared for
U.S. Department of Energy
Materials Recovery & Waste Form Development Campaign
W.L. Ebert and C.T. Snyder
Argonne National Laboratory
B.J. Riley
Pacific Northwest National Laboratory
S.M. Frank
Idaho National Laboratory

March 18, 2016

FCRD-MRWFD-2016-000038

ABSTRACT

This report describes the scientific basis underlying the approach being followed to design and develop "advanced" glass-bonded sodalite ceramic waste form (ACWF) materials that can (1) accommodate higher salt waste loadings than the waste form developed in the 1990s for EBR-II waste salt and (2) provide greater flexibility for immobilizing extreme waste salt compositions. This is accomplished by using a binder glass having a much higher Na_2O content than glass compositions used previously to provide enough Na^+ to react with all of the Cl^- in the waste salt and generate the maximum amount of sodalite. The phase compositions and degradation behaviors of prototype ACWF products that were made using five new binder glass formulations and with 11-14 mass% representative LiCl/KCl-based salt waste were evaluated and compared with results of similar tests run with CWF products made using the original binder glass with 8 mass% of the same salt to demonstrate the approach and select a composition for further studies. About twice the amount of sodalite was generated in all ACWF materials and the microstructures and degradation behaviors confirmed our understanding of the reactions occurring during waste form production and the efficacy of the approach. However, the porosities of the resulting ACWF materials were higher than is desired. These results indicate the capacity of these ACWF waste forms to accommodate LiCl/KCl-based salt wastes becomes limited by porosity due to the low glass-to-sodalite volume ratio. Three of the new binder glass compositions were acceptable and there is no benefit to further increasing the Na content as initially planned. Instead, further studies are needed to develop and evaluate alternative production methods to decrease the porosity, such as by increasing the amount of binder glass in the formulation or by processing waste forms in a hot isostatic press. Increasing the amount of binder glass to eliminate porosity will decrease the waste loading from about 12% to 10% on a mass basis, but this will not significantly impact the waste loading on a volume basis. It is likely that heat output will limit the amount of waste salt that can be accommodated in a waste canister rather than the salt loading in an ACWF, and that the increase from 8 mass% to about 10 mass% salt loadings in ACWF materials will be sufficient to optimize these waste forms. Although the waste salt composition used in this study contained a moderate amount of NaCl, the test results suggest waste salts with little or no NaCl can be accommodated in ACWF materials by using the new binder glass, albeit at waste loadings lower than 8 mass%. The higher glass contents that will be required for ACWF materials made with salt wastes that do not contain NaCl are expected to result in much lower porosities in those waste forms.

CONTENTS

FIGURES

TABLES

ACRONYMS AND ABBREVIATIONS

ACWF	Advanced Ceramic Waste Form
AFCI	Advanced Fuel Cycle Initiative
ANL	Argonne National Laboratory
ASTM	ASTM-International
CWF	Ceramic Waste Form
DIW	Demineralized Water
DOE	US Department of Energy
EBR-II	Experimental Breeder Reactor-II
EChem	Electrochemical (reprocessing)
EDS	Energy Dispersive X-ray Emission Spectroscopy
ER	Electrorefiner (salt)
FCRD	Fuel Cycle Research & Development
FCT	Fuel Cycle Technologies
HIP	Hot Isostatic Press
HLW	High-Level Radioactive Waste
ICP-MS	Inductively Coupled Plasma-Mass Spectrometry
INL	Idaho National Laboratory
MRWFD	Materials Recovery and Waste Form Development (campaign)
NBS	Sodium Borosilicate Glass
OR	Oxide Reduction (salt)
PC	Pressureless Consolidation
PNNL	Pacific Northwest National Laboratory
SEM	Scanning Electron Microscope (or Microscopy)
SLZ	Salt-loaded Zeolite 4A
ToF-SIMS	Time-of-Flight Secondary Ion Mass Spectrometry
XRD	X-ray Diffraction

ACKNOWLEDGEMENTS

The authors gratefully acknowledge technical contributions by Dr. Terry Cruse, Dr. Jeffrey Fortner, and Ms Yifen Tsai at ANL; by Ms Paula Hahn at INL; and by Dr. John Vienna, Mr. Nathan Canfield, Mr. Jared Kroll, Mr. Jacob Peterson, Mr. Jarrod Crum, and Dr. Zihua Zhu at PNNL. This report was produced under the auspices of the US DOE Fuel Cycle R&D program and Materials Recovery and Waste Form Development (MRWFD) Campaign under the direction of Dr. Terry Todd, National Technical Director, Dr. John Vienna, Deputy Manager, and Ms Kimberly Gray, DOE Federal Manager. Issuance of this report meets milestone M2FT-16AN030105071 in activity FT-16AN03010507 of WBS#1.02.03.01.05.

Work was conducted at Argonne National Laboratory and supported by the U.S. Department of Energy, Office of Nuclear Energy, under Contract DE-AC02-06CH11357.

FCRD MATERIALS RECOVERY & WASTE FORM DEVELOPMENT CAMPAIGN

Designing Advanced Ceramic Waste Forms for Electrochemical Processing Salt Wastes

1. INTRODUCTION AND BACKGROUND

The electrochemical (EChem) reprocessing methods being developed to recover and recycle uranium and plutonium from used metallic and oxide fuels generate salts that are contaminated with high-level radioactive waste (HLW) that must be removed from the electrorefiner occasionally for efficient and safe operation. The salt waste may be disposed directly or treated to remove radionuclides that must be disposed in a federal HLW repository and recycle the processing salt to the electrorefiner. A eutectic LiCl/KCl salt is used for processing metallic fuel and LiCl/Li_2O salt is used to reduce oxide fuel for further processing; these are referred to as ER and OR salts, respectively. Although direct disposal of the waste salt in a salt repository has been considered, it is likely that the waste salt or the separated waste streams will be immobilized in durable monolithic waste forms designed to meet transport, storage, and waste disposal regulations. For example, an optional processing strategy may include separating CsCl and $SrCl_2$ to produce a Cs/Sr waste form for long-term storage and separating lanthanide fission products to produce a waste form for disposal in a geological repository. Because the high Cl^- contents of these waste salts are incompatible with most waste form materials, a two-phase glass-bonded sodalite material—usually referred to as the ceramic waste form (CWF)—was developed in the 1990s to immobilize ER waste salts. In the CWF, NaCl is chemically reacted with zeolite 4A to incorporate the Cl^- into the alumino-silicate mineral sodalite, which is then microencapsulated in borosilicate glass to produce the final waste form. The small amount of oxidized fission products from the waste salt either dissolve into the glass phase or form oxide inclusions within the glass phase. The production of CWF was successfully demonstrated at the INL with salt waste generated during treatment of spent sodium-bonded nuclear fuels from the ANL Experimental Breeder Reactor-II (EBR-II) and other reactors (Federal Register 2000). The EBR-II CWF products were initially made by using a hot isostatic press (HIP) and had densities near the theoretical maximum of about 2.3 g cm^{-3} (Ebert et al. 2002). Three HIP cans with CWF could be loaded into a standard disposal canister. An alternative processing method called "pressureless consolidation" (PC) (Bateman et al. 2007) was developed in which the mixture is simply heated at ambient pressure. Although this results in waste forms with higher porosities and ~15% lower densities (Lewis et al. 2010), eliminating the volume occupied by the HIP can nearly off-sets the increased waste form volume such that similar amounts of CWF made by HIP and PC methods can be fit in a standard disposal canister.

To produce the waste form by either method, the salt-loaded zeolite 4A is mixed with crushed borosilicate glass that is used to microencapsulate the sodalite crystallites that are formed during processing. The CWF is made in two processing steps: molten salt is first occluded in zeolite 4A[1] at about 500 ºC for about 80 h to generate salt-loaded zeolite 4A (SLZ). This places these reactants in intimate contact to

[1] The material used to make CWF at INL consists of 5-µm grains of polycrystalline zeolite 4A aggregated by a clay binder and sized to –60 +200 mesh to facilitate handling in a hot cell.

facilitate the conversion reactions. The SLZ is then mechanically mixed with crushed binder glass[2]. At this point, the mixture can either be loaded into a specially designed collapsible can for HIP processing or into a canister for PC processing. For PC processing, the mixture of SLZ and glass is processed by heating to about 925 ºC for about 72 hours. The glass is sufficiently fluid at the processing temperature to infiltrate and microencapsulate the clusters of SLZ that become converted to sodalite crystallites (e.g., Richardson 1997). This produces a microstructure with variously-sized domains of sodalite crystallites embedded in a continuous glass phase. Small amounts of other phases that are present in the SLZ or form during processing become dispersed in the molten glass and are microencapsulated when the waste form is cooled. These include lanthanide and actinide elements in the salt that react with residual water in the zeolite 4A to form mixed oxides during the salt occlusion step, silicates from the clay used to aggregate the zeolite, and halite that forms during processing (e.g., Frank 2002, Morss et al. 2002a, Morss et al. 2002b). The term "glass-bonded sodalite" describes the phase composition and microstructure of the CWF.

The CWF material was identified as the baseline waste form for electrometallurgical processing salts in the review conducted by the Global Nuclear Energy Partnership [Gombert et al. 2007] and is currently the best demonstrated material available to immobilize waste salt for disposal. However, the salt waste loading in the CWF is low (about 8 mass %) and waste form production is fairly complex and time consuming. Work is in progress under the auspices of the DOE Fuel Cycle Technologies R&D program to develop "advanced" CWF materials that have higher waste loadings, can accommodate a wider range of waste salt compositions, and can be produced more efficiently than the CWF developed for EBR-II salt waste.

Zeolite 4A reacts with NaCl in the salt to form sodalite, but reacts with other alkali metal chlorides to form aluminosilicates that do not contain Cl^-. The low Na^+ contents of most waste salts limits the amount of sodalite that can be produced. Evidence generated in laboratory tests that are summarized in this report indicates the binder glass participates chemically in the conversion reaction through the exchange of Na^+ with cations from the salt. Note that we write Na^+ to emphasize the participation of the oxidized species in the reactions rather than metallic Na. Based on the reactions occurring to generate the CWF, it was hypothesized that the salt waste loading could be increased significantly by using the binder glass to provide additional Na^+ to sequester more Cl^- and balancing the stoichiometries of the reactions that produce sodalite to accommodate the Cl^- with the relative amounts of salt, zeolite 4A, and binder glass that are used to produce the CWF.

Besides encapsulating sodalite in a physically durable monolithic waste form, the glass phase in the CWF serves three other important purposes: (1) it encapsulates the micron-sized lanthanide and actinide oxides that are produced during the occlusion step and the halite inclusions that form when the waste form is processed; (2) Na^+ from the glass is exchanged with other alkali metal and alkaline earth cations in the salt (including and most importantly fission products), which allows them to be incorporated into the glass structure; and (3) the Na^+ provided by the glass reacts with Cl^- in the salt and zeolite 4A to form sodalite or halite. Furthermore, the physical, radiological, and chemical durability of the waste form is provided by glass phase. This is because glass dissolution controls the releases of those radionuclides that are chemically dissolved within the glass and the rate at which water contacts the other radionuclide-bearing phases that are physically encapsulated by the glass. The inclusion phases may contribute to the waste form durability.

[2] The term "binder glass" is used to differentiate the reagent glass used to make CWF materials from the glass phase that results after processing the CWF.

1.1 Development of the CWF

Development of the CWF has occurred in three "eras". The initial development in the 1990s resulted from empirical studies to identify an appropriate borosilicate glass to encapsulate the sodalite. The production method included a salt occlusion step in which zeolite 4A was soaked in molten salt so waste constituents would diffuse into the atomic-scale pore structure of the zeolite. This step was thought to place radionuclides within the zeolite 4A pores and trap them within the slightly smaller pore structure of sodalite when it formed. The role of the glass was to encapsulate the sodalite that formed. Production of CWF materials utilized separate steps to efficiently occlude the salt in the zeolite 4A, mix the SLZ with glass frit, then process the mixture to convert the SLZ to sodalite and encapsulate the sodalite in the glass. Analyses of CWF products[3] made with different mixtures and under different conditions showed small amounts of halite (NaCl) and nepheline ($NaAlSiO_4$) were often formed along with sodalite. Processing conditions were controlled to limit the amount of non-occluded (free) salt that remained after producing the SLZ and the amounts of halite and nepheline in the CWF product. This resulted in a conservative formulation of the CWF with a low salt waste loading of about 8 mass %. At the same time, use of a hot isostatic press was abandoned and replaced by a pressureless consolidation method in which the CWF is produced as a 450-kg monolith that is densified only under its own weight. This results in a CWF product that has a slightly higher porosity than those made with HIP, but materials made by the HIP and PC methods have similar microstructures and chemical durabilities. Three full-size PC CWF products can be stacked in a standard (short) disposal container.

The second era occurred during testing and modeling activities in the 2000s to support including CWF in the DOE license application to construct the Yucca Mountain repository. Detailed analyses of CWF products revealed that radionuclides were not "trapped" in sodalite cages, the general size of the sodalite domains matched the size of the aggregated zeolite (and the SLZ), and glass had penetrated into the domains sodalite to microencapsulate the individual micrometer-sized sodalite crystallites. The composition of glass between the sodalite grains (which is sometimes referred to as intergranular glass) was significantly depleted of Na and enriched in K. Scoping tests were conducted to evaluate the capacity of CWF products to accommodate higher salt waste loadings by varying the salt loading in the SLZ, the salt composition, and the relative amounts of P57 glass and SLZ. The relative amounts of halite and nepheline that were formed and the chemical durabilities of the resulting products indicated that acceptable CWF waste forms could be made with higher salt waste loadings. The finding that the halite inclusions did not contain measurable concentrations of salt cations other than Na indicated they were not formed of unreacted waste salt. Trace amounts of iodide were detected in the halite inclusions and sodalite in the same proportion as Cl^-. Scoping experiments conducted to evaluate the flexibility of CWF products to accommodate salt compositions with high Cs contents indicated other mineral phases could be generated (Cs-pollucite in that case) in addition to sodalite. Research to further develop the CWF was halted and the work continued at INL was focused on producing full-size CWF products. Although most of the research to develop the CWF was considered applied technology and is not publically available, a summary report was approved for public release and issued (Ebert 2005).

The third era of development instigated in the 2010s based on hypotheses developed in 2007 when use of CWF-type products was being evaluated as a possible waste form for additional waste streams under the DOE AFCI program. The CWF was identified as the baseline waste form for electrometallurgical processing salts enriched in lanthanides and other fission products in the review conducted within the Global Nuclear Energy Partnership (Gombert et al. 2007). Development of CWF-type products is continuing under the auspices of the Fuel Cycle Research & Development (FCRD) program (Ebert and Snyder 2015). Note that the use of tellurite glasses has been evaluated as an alternative to CWF-type

[3] The term "products" is used to distinguish CWF materials formulated and produced to represent waste forms from materials made to study the processing steps.

products for immobilizing salt wastes (e.g., Riley et al. 2012, McCloy et al. 2013, Riley et al. 2015, Ebert and Snyder 2015). Further development of tellurite-based waste forms is not being pursued by DOE and the CWF remains the best demonstrated waste form for immobilizing LiCl/KCl-based salt wastes. Two major objectives of the current research are to increase the salt waste loading that can be achieved in an acceptable waste form for various waste salt compositions and improve the efficiency of the production method. Based on the status summarized in this report, we believe the capacity of CWF waste forms to accommodate LiCl/KCl-based salt wastes has been optimized and further studies to develop and evaluate alternative production methods are justified. We refer to the optimized materials as "advanced" ceramic waste form (ACWF) products because a reformulated glass binder is utilized as a reactant to increase the salt waste loading rather than simply to encapsulate the sodalite. An important anticipated benefit of this approach is that ACWF materials can be used with a wider range of waste salt compositions. This is discussed in Section 2.

1.2 The Chemistry Behind CWF Production

The primary role of the sodalite phase in the waste form is to host the chloride ions in the waste salt so the radionuclide cations can dissolve in the glass. The reaction to form sodalite is

$$\underset{\text{zeolite 4A}}{Na_{12}(AlSiO_4)_{12}} + 4\ NaCl \rightarrow 2\ \underset{\text{sodalite}}{Na_8(AlSiO_4)_6Cl_2}\,. \qquad \text{Reaction 1}$$

For materials made with an amount of NaCl exceeding this stoichiometry, the amount of halite that will be generated can be calculated as

$$\text{moles excess halite} = \text{NaCl per formula SLZ} - 4 \qquad \text{Reaction 2}$$

where the value of 4 is for stoichiometric transformation of SLZ to sodalite. In practice, the salt is occluded in the zeolite 4A to generate SLZ to facilitate Reaction 1. Although the CWF developed for EBR-II salt was formulated with a substoichiometric amount of salt to prevent generation of halite inclusions in the waste form, nepheline and halite can be generated as decomposition products:

$$\underset{\text{sodalite}}{Na_8(AlSiO_4)_6Cl_2} \rightarrow 2\ NaCl + 1.5\ \underset{\text{nepheline}}{Na_4(AlSiO_4)_4}\,. \qquad \text{Reaction 3}$$

The target salt loading in the SLZ used for the EBR-II CWF was 10.7 mass% salt (Ebert et al. 2005). That salt composition provided 3.8 NaCl per formula SLZ and 0.15 moles of nepheline were formed per formula:

$$\underset{\text{zeolite 4A}}{Na_{12}(AlSiO_4)_{12}} + 3.8\ NaCl \rightarrow \underset{\text{SLZ}}{Na_{12}(AlSiO_4)_{12}\bullet 3.8\ NaCl} \qquad \text{Reaction 4}$$

$$\underset{\text{SLZ}}{Na_{12}(AlSiO_4)_{12}\bullet 3.8\ NaCl} \rightarrow 1.90\ \underset{\text{sodalite}}{Na_8(AlSiO_4)_6Cl_2} + 0.15\ \underset{\text{nepheline}}{Na_4(AlSiO_4)_4} \qquad \text{Reaction 5}$$

Whereas the formation of nepheline is detrimental to HLW glasses because it removes equal amounts of Al and Si from the neighboring glass, which decreases its chemical durability (e.g., Li et al. 1997), the binder glass is not the source of the Si and Al consumed by nepheline formation in the CWF and the formation of nepheline is not detrimental to the glass durability. However, the formation of nepheline consumes zeolite 4A and decreases the amount of sodalite that can form and, therefore, the amount of waste salt that is immobilized.

The formation of halite inclusions is not detrimental to the chemical durability of the CWF because it does not significantly affect the glass composition or waste form performance because the halite inclusions only contain trace amounts of iodine. However, inclusions of the waste salt that may be generated in an improperly-formulated waste form will be detrimental to the waste form performance owing to the high radionuclide content of unreacted salt.

1.3 Salt Waste Loading in the CWF

The radionuclide content of CWF products is determined by the radionuclide content of the salt and the salt waste loading in the waste form. The maximum salt waste loading that can be achieved is determined by the Cl^- content of the salt, the relative amounts of NaCl and zeolite-4A available to react, and the amount of glass required to encapsulate the sodalite and other phases that are generated during processing. Other factors include the capacity of the glass phase to exchange Na with other cations in the salt. Other than sodalite, the two most abundant inclusion phases are halite formed from excess NaCl and mixed oxides of lanthanides and actinides that form when the salt is occluded in the zeolite during the salt loading step. The maximum waste loading is usually limited by the chloride content of the salt and the amount of Na available in the system to generate enough sodalite to accommodate the chloride in the salt. The latter is determined by the NaCl content of the salt and Na_2O content of the binder glass. Alkali metals in the salt other than Na are not effective in generating sodalite and instead exchange with Na in the glass or form other phases (e.g., Cs-pollucite and Li-aluminosilicate), depending on their concentrations. The Na released from the glass by ion exchange is consumed by formation of sodalite or halite. The Na content of the glass must be adequate to accommodate exchange with the other cations in the salt unless another phase is formed. The Na contents of the salt and glass establish a maximum waste loading above which sufficient sodalite and halite cannot be formed to immobilize the waste salt. Alternative waste forms utilizing other mineral phases to accommodate waste cations such as Cs and Sr in waste salts that do not generate sodalite have been proposed to avoid unacceptably large amounts of residual radionuclide-bearing salt being distributed throughout the waste form. Waste loadings with these salts will be significantly lower because these phases do not accommodate Cl^- and must be formed in addition to sodalite.

The 8 mass% salt waste loading formulated for EBR-II waste (10.7% salt in the SLZ and 75% SLZ in the CWF) is unnecessarily low. That waste salt contained about 6.8 mol% Na and 51.1 mol% Cl^- such that every 10 g of salt provided 0.170 moles Cl^- and 0.227 moles Na. An additional 1.31 g of Na was required to produce enough sodalite to accommodate all of the Cl^- in the waste salt; that Na was acquired from the glass. The binder glass P57 that was used to make the CWF during the developmental phase contained 5.23 mass% Na, so 33 g of that glass could provide 1.73 g Na^+ to react with the zeolite 4A and salt. Theoretically, the 0.43 g of Na (0.019 moles) that remain in the glass phases of CWF products made with P57 glass could have been removed from the glass by ion exchange to accommodate an additional 1% waste salt. Consistent with this expectation, the composition of the glass between sodalite grains in reference CWF products have been found to be significantly depleted in Na (O'Holleran 1999; Frank 2004).

The stoichiometry of the reaction converting zeolite 4A to sodalite can be used to formulate CWF materials with higher waste loadings as follows. Chloride typically represents about 60 mass% of the waste salt. For CWF made with the stoichiometric amount of NaCl loaded in the zeolite and the reference amounts of SLZ and glass, the masses of NaCl , zeolite, glass, and CWF can be related to the mass of Cl^- in the salt based on the stoichiometries of the reactions and the nominal ratios of salt:zeolite:glass used in the CWF formulation (which is 8:67:25) as follows. The mass fraction of Cl^- in sodalite is 0.07316, so 13.67 g of sodalite is required to sequester each gram of Cl^- in the salt. Based on the stoichiometry in

Reaction 1, every gram of Cl^- in the salt requires 12.02 g zeolite 4A to react with 1.648 g NaCl to make 13.67 g sodalite. For a CWF product made with 25 mass% glass[4], the mass of SLZ is 3-times the mass of glass. The stoichiometric amounts of zeolite and glass can be calculated based on the mass of Cl^- by using the following proportionalities:

$$\text{mass zeolite 4A} = 12.02 \times \text{mass } Cl^- \quad (1)$$

$$\text{mass NaCl} = 1.648 \times \text{mass } Cl^- \quad (2)$$

$$\text{mass glass} = (\text{mass SLZ})/3 = (\text{mass zeolite 4A} + \text{mass NaCl})/3 = 4.556 \times \text{mass } Cl^- \quad (3)$$

$$\text{mass CWF} = \text{mass NaCl} + \text{mass zeolite 4A} + \text{mass glass} = 18.22 \times \text{mass } Cl^- \quad (4)$$

For example, if 60 g of Cl^- is present in 100 g of salt, that salt will be accommodated stoichiometrically in 820 grams of sodalite. Generation of this amount of sodalite requires 721.1 g zeolite 4A and 98.9 g NaCl. The 820 g of SLZ is mixed at a 3:1 ratio with 273.3 g glass to make 1093 g of CWF. The salt waste loading is 9.1%. Note that the stoichiometric relationships are with the amount of Cl^- in the salt, not with the salt itself. The relationships between Cl^-, zeolite 4A, and sodalite (in Equations 1 and 2) are fixed by stoichiometry, whereas salts with different Cl^- contents and CWF made with different ratios of glass and SLZ (in Equation 3) will result in slightly different waste loadings expressed with respect to the salt. For example, using only 20 mass% binder glass to encapsulate the sodalite in the above example gives a salt waste loading of 9.8%; this may not be enough glass to completely encapsulate the sodalite. Further increases in the waste loading require the formation of halite inclusions to accommodate some of the Cl^- by using less than the stoichiometric amount of zeolite 4A but the same amount of Na^+. Production of CWF products assumes the stoichiometric amount of Na^+ is available for reaction with all of the Cl^- in the salt. Waste salt compositions will always contain far less Na^+ than Cl^- and require additional Na to be extracted from the binder glass.

It is important to note that the P57glass used to develop and qualify EBR-II CWF is no longer available commercially and that an alternative glass with one-third the Na content (2.3% Na_2O compared to 6.9 % Na_2O) is now being used at INL (Bateman et al. 2007). Although that glass was shown to be adequate for the EBR-II formulation, the low Na_2O content of this glass will probably limit the amount of sodalite that can be generated and the waste loadings that can be achieved for salts with low NaCl contents.

Contaminants (represented as chlorides) comprise about 27 mass% of the reference waste salt; the upper limit to the contaminant concentration in processing salt is estimated to be about 35 mass% (Frank, 2014). It is likely that the relative amounts of Na^+ and Cl^- in the waste salt will decrease proportionally as the contaminant concentrations increase, and that the primary impact will be greater amounts of contaminants that must dissolve into the binder glass. This will require more Na to be provided by the glass to exchange with cations in the salt and probably affect the relative amounts of sodalite and halite that form. However, less sodalite will be required to accommodate the lower fraction of Cl^- in the salt, and the salt loading can be decreased while the radionuclide loading increases. The relationships in Equations 1-4 will change accordingly. Recent calculations by Vienna (2015) suggest waste forms made with 12% waste loadings of the nominal ER salt wastes that are cooled 50 years before disposal will meet expected thermal limits for disposal in clay or shale-based disposal systems. However, lower salt waste loadings may be required for waste salts with high Cs-137 or Sr-90 concentrations to meet thermal limits of the disposal system.

[4] The densities of sodalite and the borosilicate glasses used to make CWF products are sufficiently similar that mass fractions are used to approximate volume fractions.

Although the role of the waste form is to immobilize radionuclides rather than immobilizing NaCl, the Cl^- content of the waste salt and the amount of NaCl available to generate sodalite limits the radionuclide contents that can be achieved in these waste forms. The majority of the waste form volume is dedicated to the sodalite required to sequester Cl^-. Most radionuclides are present in the waste form as micrometer-sized inclusion phases encapsulated by the glass (lanthanides and actinides) or dissolved in the glass (alkali metal and alkaline earth fission products). Figure 1 provides representative optical and TEM photomicrographs showing clusters of inclusion phases in the glass near a sodalite domain. Most of the oxide phases are generated when the salt is occluded in the zeolite 4A and halite is generated during waste form processing (e.g., by Reaction 3). When EBR-II CWF products are made with surrogate waste salt, which is predominately a mixture of LiCl, NaCl, and KCl, the excess salt that is not consumed by sodalite formation migrates out of sodalite regions and into the molten glass as an immiscible liquid phase.

As the waste form cools, the glass solidifies first and the droplets of molten salt remain as spherical inclusions in the glass. The salt crystallizes as halite within spherical voids in the glass as the waste form cools. The included phases are physically retained by the glass (not chemically) and may become transportable as the glass corrodes and the inclusion phases are contacted by water. Halite inclusions will dissolve rapidly when contacted by water, but most oxide inclusions are sparingly soluble and can likely only be transported as colloids by advection after the surrounding glass has dissolved. In general, the performance of the CWF and ACWF in retaining radionuclides will be determined by the chemical durability of the glass phase. The approach proposed previously for representing the CWF in a disposal system performance assessment calculations by using the defense high-level waste glass model (Ebert 2005) can also be used for ACWF products and a similar suite of tests to support modeling can be applied to representative materials when they are developed.

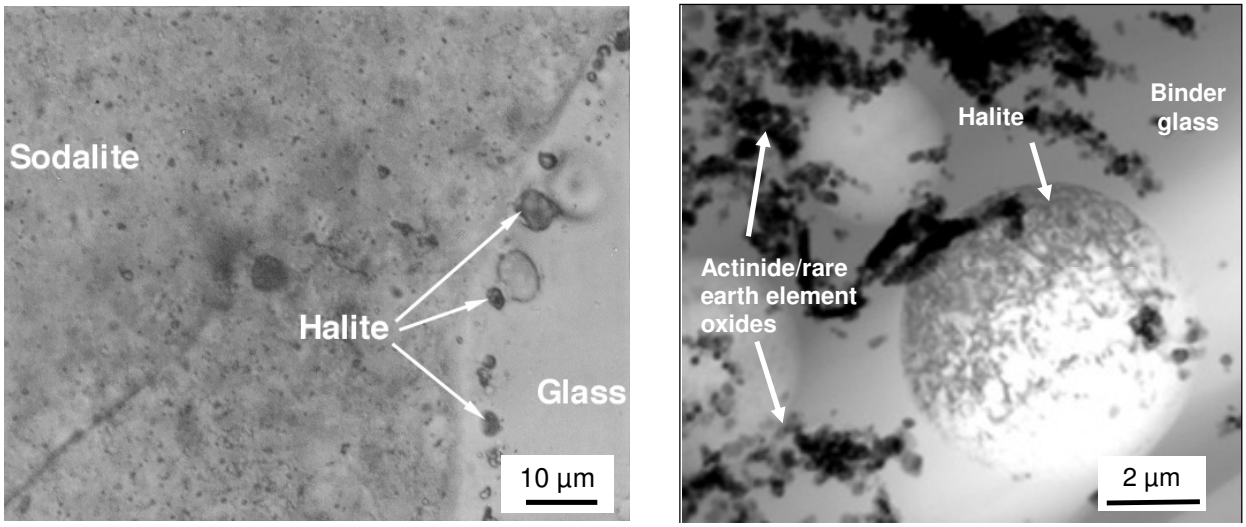

(a) (b)

Figure 1. (a) Optical photomicrograph and (b) TEM photomicrograph showing halite and oxide inclusion phases in the glass phase of a CWF product near a sodalite domain.

2. SALT WASTE COMPOSITIONS

The results of a scoping study conducted during FY2005 as part of the EBR-II spent fuel treatment project to evaluate the effects of salt loading and glass content on the physical and chemical integrity of CWF products (Ebert et al. 2005) indicated (1) that acceptable waste forms could probably be produced with salt waste loadings in the SLZ increased from 10.7 to 15 mass% and the glass content decreased from 25% to 20% to achieve an over-all salt loading of about 12 mass%; (2) that the generation of additional phases (such as halite and nepheline) will not necessarily result in an unacceptable waste form, and (3) that a lower salt loading (3.75% in the CWF) resulted in a slightly less durable but probably a acceptable waste form. Although the highest acceptable waste loadings are desired, it is important that waste forms made with lower waste loadings due to processing variances are also acceptable. Whereas the total Cl^- content of the salt determines the amount of sodalite required to sequester it, the availability of Na^+ limits the amount of sodalite that can be produced.

Analyses of standard CWF products indicate that essentially all of the Na can be removed from the glass during processing (O'Holleran 1999; Frank 2004). Since the waste salt provides only about 10% of the Na^+ needed to immobilize all of the Cl^- within sodalite, it has been hypothesized that a binder glass having a higher Na_2O content can be used to achieve higher salt waste loadings in durable waste forms. The Na removed from the glass is replaced by cations from the salt to maintain charge neutrality. This also incorporates the radionuclides into the glass structure.

2.1 Nominal Compositions of Salt Waste

A representative composition of discharged ER salt wastes from electrometallurgical treatment and the theoretical waste stream compositions after efficient separation of lanthanides are given in Table 1. This gives the theoretical composition of waste salt after processing 300 driver assemblies of EBR-II sodium-bonded fuel, and is referred to as "300 driver salt". The lanthanides, actinides, active metals, and eutectic salt comprise about 13.7%, 9.8%, 16.9%, and 59.7% of the total mass, respectively. It is anticipated that (1) actinides (and perhaps rare earth elements) will be recovered from the salt and (2) Ba, Cs, Sr, and Rb (and perhaps rare earth elements) will be highly concentrated in the salt relative to their concentrations in the waste salt removed from the electrorefiner. Several methods for concentrating the waste components in the salt are being investigated, including precipitation and sorption methods, and the range of concentrations that may occur in the waste salts is not known. From the predicted salt composition CsCl, $BaCl_2$, and $SrCl_2$ will play important roles in determining the phase composition of glass-bonded mineral waste forms made with FCRD waste salts. The reactivities of these salts with zeolite 4A and glass are not known, but the reactions to form mineral phases or dissolve in the glass are expected to impact the production and performance of ACWF materials. Insights and expectations based on previous studies are discussed in the following sections.

2.2 CsCl-Enriched Salt Waste

Lambregts and Frank (2002, 2003) prepared CWF products using either 100% CsCl, a mixture of 50% CsCl and 50% NaCl, or a mixture of 25% CsCl and 75% NaCl instead of the surrogate waste salt to study the disposition of Cs in the various phases. The analysis of these materials provides valuable insight into the likely disposition of Cs in waste forms made with FCRD waste salts that are enriched in CsCl. All three materials were processed at 915 °C for 4 h and are referred to herein as Cs-CWF products to distinguish them from CWF products made with surrogate ER salt. The salt waste loadings of the CsCl:NaCl mixtures occluded in zeolite 4A were the same as the nominal loading of the surrogate ER salt

Table 1. Estimated salt waste stream compositions for discharged waste salt and after removing lanthanide and actinide salts

		Discharged Salt[a]		After Actinide and Lanthanide Removal			
	Component	mole	mass (g)	mole	mole%	mass (g)	mass%
Lanthanide Salts	YCl_3	2.006	391	—	—	—	—
	$LaCl_3$	8.247	2021	—	—	—	—
	$CeCl_3$	12.565	3104	—	—	—	—
	$PrCl_3$	6.124	1513	—	—	—	—
	$NdCl_3$	18.85	4727	—	—	—	—
	$PmCl_3$	0.713	180	—	—	—	—
	$SmCl_3$	5.537	1409	—	—	—	—
	$EuCl_3$	0.672	174	—	—	—	—
	$GdCl_3$	0.606	159	—	—	—	—
	$TbCl_3$	0.046	12.3	—	—	—	—
Actinide Salts	UCl_3	10.25	3502	—	—	—	—
	$NpCl_3$	0.762	262	—	—	—	—
	$PuCl_3$	15.47	5342	—	—	—	—
	$AmCl_3$	1.541	534	—	—	—	—
	$CmCl_3$	0.401	142	—	—	—	—
Active Metal Salts	NaCl	176.7	10318	176.7	13.76	10320	13.45
	RbCl	1.779	216	1.779	0.14	216.3	0.28
	$SrCl_2$	3.747	598	3.747	0.29	598.8	0.78
	CsCl	20.47	3482	20.47	1.59	3482	4.54
	CsI	2.114	549.2	2.114	0.16	549.2	0.72
	$BaCl_2$	8.520	1776	8.520	0.66	1776	2.32
Eutectic Salts	LiCl	621.8	26300	621.8	48.42	26300	34.28
	KCl	449.3	33470	449.3	34.98	33470	43.63
	Total	*1368*	*100200*	*1284*	100	*76720*	100

[a]Salt composition after processing used sodium-bonded fuel from 300 EBR-II driver assemblies.

on a molar basis (i.e., about 0.13 moles salt per 100 g CWF). The salt loadings in these materials was not reported, but are all presumed to be about 8 mass%. These Cs contents are about 25-, 19-, and 6-times higher than the Cs contents in the nominal CWF products with EBR-II salt.

As has been observed for other CWF products, Cs did not substitute for Na to form a Cs-sodalite phase. Instead, both Cs-pollucite and Cs-free sodalite formed in the materials made with the 100CsCl:0NaCl and 50CsCl:50NaCl salt mixtures; only Cs-free sodalite formed in the material made with the 25CsCl:75NaCl salt mixture. Photomicrographs from scanning electron microscope (SEM) examinations by Lambregts and Frank (2002) and Lambregts and Frank (2003) are reproduced in Figure 2. Despite the poor quality of the reproduction, the formation of separate phases is clearly seen and shows that the glass failed to encapsulate the other phases. The darkest areas are epoxy used to make the cross section. The small bright spots distributed in the sodalite domains[5] formed in the Cs-CWF materials that were made with the 100CsCl:0NaCl mixture are Cs-pollucite; fewer regions of Cs-pollucite were detected in the Cs-CWF made with the 50CsCl:50NaCl and 25CsCl:75NaCl salt mixtures. Trace amounts of halite were detected in all three materials by using NMR, but CsCl was not detected (Lambregts and Frank 2003).

[5] The term "sodalite domain" refers to the clusters of sodalite crystallites in the CWF that have retained the arrangement of the zeolite 4A grains in the aggregates from which they formed.

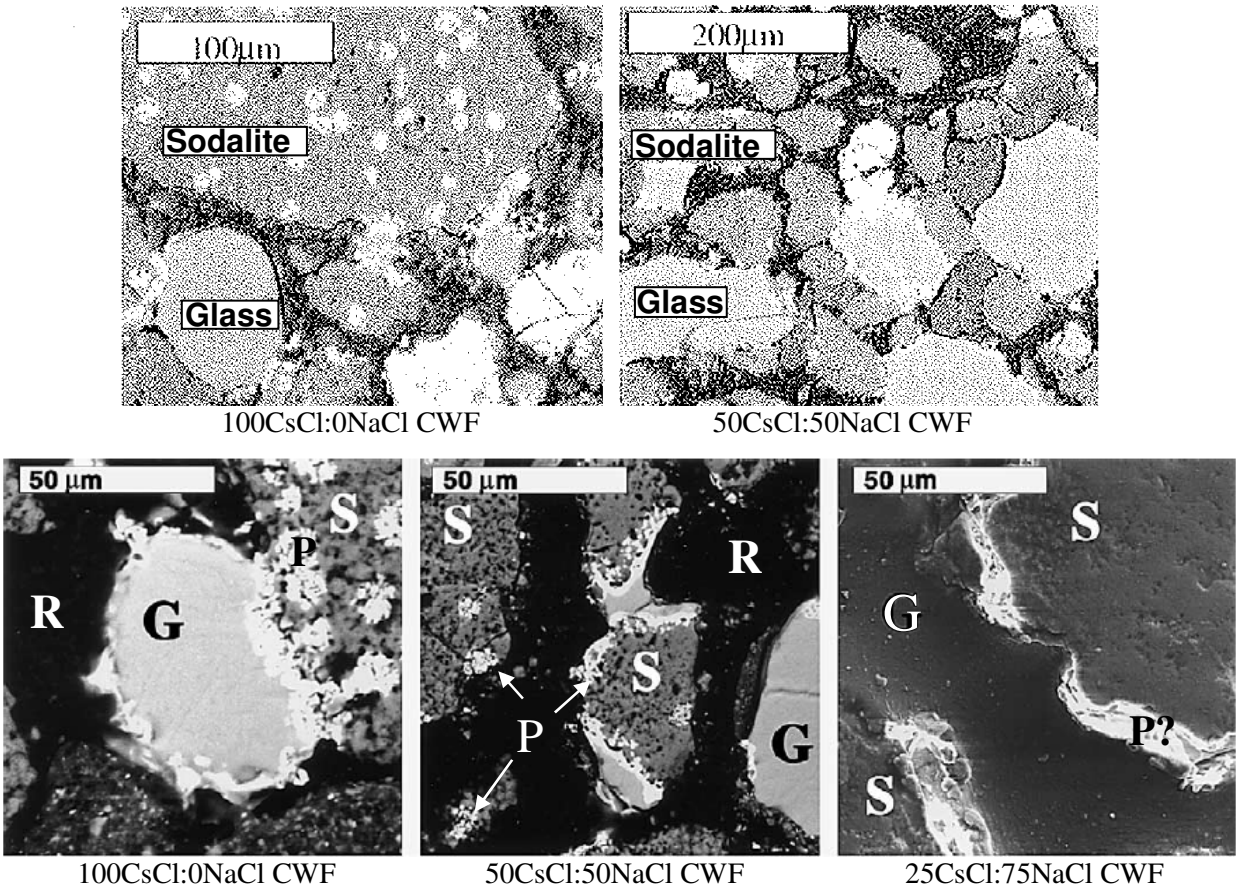

Figure 2. SEM photomicrographs of Cs-CWF reproduced from (a) Lambregts and Frank (2002) and (b) Lambregts and Frank (2003). S = Sodalite, G = Glass, P = Cs-pollucite, R = Resin.

The materials made by Lambregts and Frank (2002) indicate zeolite 4A reacts in parallel reactions with CsCl to form Cs-pollucite and with NaCl to form of sodalite. The formation of Cs-pollucite requires additional silica, which could be provided by the molten glass, according to the net reaction

$$\underset{\text{zeolite 4A}}{Na_{12}(AlSiO_4)_{12}} + 12\ \underset{\text{salt}}{CsCl} + 12\ \underset{\text{glass}}{SiO_2} \rightarrow 12\ \underset{\text{Cs-pollucite}}{CsAlSi_2O_6} + 12\ \underset{\text{halite}}{NaCl}. \qquad \text{Reaction 6}$$

The NaCl that is generated could react with zeolite 4A to form sodalite following Reaction 1. The combination of Reactions 1 and 6 gives Reaction 7

$$4\ \underset{\text{zeolite 4A}}{Na_{12}(AlSiO_4)_{12}} + 12\ \underset{\text{salt}}{CsCl} + 12\ \underset{\text{glass}}{SiO_2} \rightarrow 6\ \underset{\text{sodalite}}{Na_8(AlSiO_4)_6Cl_2} + 12\ \underset{\text{Cs-pollucite}}{CsAlSi_2O_6}. \qquad \text{Reaction 7}$$

Reaction with NaCl does not consume silica

$$3\ \underset{\text{zeolite 4A}}{Na_{12}(AlSiO_4)_{12}} + 12\ NaCl \rightarrow 6\ \underset{\text{sodalite}}{Na_8(AlSiO_4)_6Cl_2}. \qquad \text{Reaction 8}$$

Reactions 7 and 8 are written with stoichiometries for the reactions of equal molar amounts of CsCl and NaCl to facilitate comparisons. Lambregts and Frank (2003) found that increasing the fraction of NaCl in the salt mixture increased the fraction of sodalite and decreased the fraction of Cs-pollucite generated in the CWF. Increasing the amount of Na available from the glass is likewise expected to decrease the fraction of Cs-pollucite by promoting Reaction 7 to form sodalite.

The high Cs contents clearly affected the assemblages of phases that formed and the Cs distributions in the materials made with the 100CsCl:0NaCl and 50CsCl:50NaCl salt mixtures. Some of the Cs was dissolved into the glass and some was sequestered in Cs-pollucite. An additional Cs-bearing phase that appears to have formed as small inclusions within sodalite domains of the materials was identified as "low form cesium ANA" by Lambregts and Frank (2003). They detected NaCl (halite) by using nuclear magnetic resonance (NMR) spectroscopy, but did not detect CsCl and Cs was not detected in the sodalite. The sizes of the halite inclusions formed in CWF are typically on the order of 1-micrometer. The microstructures of the Cs-CWF products shown by Lambregts and Frank (2002) also differed from EBR-II CWF materials made with surrogate waste salt in that the glass phase was not continuous in either material and did not encapsulate the other phases.

Of course, the consumption of SiO_2 to form Cs-pollucite will impact the amount of glass that remains and its properties. As stated above, dissolution of cations from the salt into the glass is required to provide the Na^+ needed to form sodalite and immobilize the Cl^- from the salt. The dissolution of zeolite 4A into the glass could also supply the SiO_2 required to form Cs-pollucite and Na_2O to form sodalite, but would simultaneously increase the Al_2O_3 contents of the glass. That was not observed (see below) and the dissolution of zeolite 4A into the glass is not considered to be significant.

The composition of the glass phases in the Cs-CWF materials measured by Lambregts and Frank (2002) indicated that the Na content of the glass decreased from about 5 mass% to less than 1 mass%, the Si content remained near 30 mass%, and the Cs concentration in the glass increased from none to about 17 mass%. Small amounts of halite were detected by Lambregts and Frank (2003), but CsCl was not detected. These results suggest ion exchange occurred between Na^+ in the glass and Cs^+ in the small amounts of CsCl that were not sequestered in Cs-pollucite to incorporate Cs^+ into the glass phase:

$$\text{Na-O-Si}\equiv\text{glass} + \text{CsCl} \rightarrow \text{Cs-O-Si}\equiv\text{glass} + \text{NaCl}. \qquad \text{Reaction 9}$$

The first term on the left hand side of the reaction in Reaction 9 represents Na associated with a non-bridging oxygen in the glass by a mostly ionic bond. This Na^+ exchanges with Cs^+ from the salt to form NaCl, which can then react with zeolite 4A to form sodalite, and Cs bonded to the non-bridging oxygen in the glass (i.e., Cs dissolved in the glass). The amount of Cs dissolved in the glass will depend on the equilibrium and kinetics of Reaction 9 and the relative amounts of sodalite and Cs-pollucite that form by consuming NaCl and CsCl, respectively. The absence of detectable amounts of CsCl in the CWF made by Lambregts and Frank suggests the equilibria for Reactions 7 and 9 both lie far to the right. The fact that they only detected trace amounts halite (NaCl) inclusions in the Cs-CWF materials indicates that essentially all of the NaCl was consumed by the generation of sodalite.

Finally, it is expected that only a small amount of CsCl in the salt penetrated into the interior of the zeolite 4A in the salt-occlusion step, and that most remained near the outer surface. Reaction to form Cs-pollucite in the interior of the aggregated zeolite was fairly localized and resulted in small crystals. The CsCl at the outer surface was more mobile and formed larger Cs-pollucite phases outside the sodalite domains. Although the relative amounts of sodalite and Cs-pollucite formed in each material were not quantified, it appears in the photomicrographs presented in Lambregts and Frank (2002) that more Cs-pollucite was formed in the Cs-CWF made with the 100CsCl:0NaCl salt mixture (100% Cs) than in the Cs-CWF made with the 50CsCl:50NaCl salt mixture. Because the formation Cs-pollucite consumes a

significant fraction of the glass, more than 20 mass% binder glass must be added to make a robust waste form with waste salts having high CsCl contents.

The composition of the localized glass domains provides useful insight into the stoichiometry of the phases and capacity of the glass phase to accommodate dissolved Cs. The compositions of the glass phases of the Cs-CWF materials made with the different salt mixtures that were measured by Lambregts and Frank (2003) with energy dispersive x-ray emission spectroscopy (EDS) are summarized in Table 2. The concentrations are normalized to 100%, even though boron is known to be present in the glass phase, but the analysis does not detect B. The Cs content of the glass increases and the Na content decreases as more CsCl and less NaCl is added to the Cs-CWF. This is interpreted to indicate some of the Na in the glass exchanged with Cs from the salt. The Al/Si ratio of the glass in the Cs-CWF made with the 25CsCl:75NaCl salt mixture was higher than that ratio in the reagent glass, but the ratios for Cs-CWF made with the 50CsCl:50NaCl and 100CsCl:0NaCl salt mixtures were about the same as that for the reagent glass. Although the ratio is expected to increase as zeolite 4A dissolves in the glass and as Si (but not Al) is removed from the glass to form Cs-pollucite, essentially the same Al/Si ratio was measured in the glass after Cs-pollucite formed in the Cs-CWF made with the 100CsCl:0NaCl and 50CsCl:50NaCl salt mixtures (the differences are all within the analytical uncertainty). Note that the Al/Si ratio measured in the Cs-CWF made with the 25CsCl:75NaCl salt mixture, which is 0.30, is similar to that for the theoretical glass composition if 23.6 mass% of the zeolite 4A had dissolved into the glass, which is 0.37.

Although it was not quantified, far less glass appears to remain in the Cs-CWF materials than the typical CWF. Based on the photomicrographs published by Lambregts and Frank, the binder glass did not encapsulate the crystalline phases in the CWF materials made with either the 100:0 or 50:50 salt mixture. However, the microstructure of the Cs-CWF made with the 25:75 salt mixture is similar to that of the nominal CWF, probably due to the high Na content of that salt mixture. By replacing the surrogate salt with an equimolar amount of the CsCl/NaCl mixture, Lambregts and Frank added more CsCl than could be accommodated by the formation of Cs-pollucite, but excess CsCl was not detected. Instead, a significant amount of Cs was dissolved into the glass, which probably occurred by exchange with Na in the glass by the reaction given in Reaction 9.

Lambregts and Frank did not report the actual amounts of Cs used to make the CWF materials. Instead, they stated that "Appropriate amounts of the salts and dry zeolite 4A were transferred…" and "…samples were mixed with borosilicate glass…at a 3:1 SLZ to glass ratio by weight" (Lambregts and Frank 2002). Assuming the Cs:Na mixtures used by Lambregts and Frank were formulated to provide 0.134 moles of Cl^- in total, the 50CsCl:50NaCl salt mixture provided 0.067 moles of CsCl and 0.067 moles of NaCl and the 25CsCl:75NaCl mixture provided 0.0335 moles of CsCl and 0.1005 moles of NaCl. The 100CsCl:0NaCl salt mixture provided 0.134 moles of CsCl. The 0.0393 moles in 67 g of

Table 2. Measured compositions of glass phases in various Cs-CWF materials

	mass%[a]					mole ratio	
Material	Na	Cs	Al	Si	O	Cs/Na	Al/Si
100CsCl:0NaCl	0.89	17.1	3.54	30	48.2	3.3	0.12
50CsCl:50NaCl	1.4	14.3	3.88	31.3	49.2	1.8	0.13
25CsCl:75NaCl	4.26	9.35	10.5	35.8	39.5	0.38	0.30
Reagent glass[b]	5.21	0	4.26	31.8	58.7	0	0.14

[a]Lambregts and Frank 2003 Table 1.
[b]Compositions in Table 5 renormalized to include only Al, Na, Si, and O for comparison.

zeolite 4A can react with 0.1572 moles of NaCl to form sodalite according to Reaction 1 *or* with 0.1179 moles of CsCl to form Cs-pollucite according to Reaction 6. If 15% of the zeolite 4A dissolves into the glass, the remaining 0.0334 moles of zeolite 4A can react with 0.1336 moles of NaCl to form sodalite by Reaction 1 *or* with 0.1002 moles of CsCl to form Cs-pollucite by Reaction 6.

The charge of 100CsCl:0NaCl salt mixture used to make the Cs-CWF material provided more CsCl than could be accommodated by reaction with all of the available zeolite. While some of the CsCl reacted to form Cs-pollucite, an appreciable amount of Cs was exchanged with Na in the binder glass to form NaCl, which then reacted with some of the zeolite 4A to form sodalite. Although all the CsCl in the charges of the other salt mixtures *could* have been accommodated by formation of Cs-pollucite, the detection of significant amounts of Cs in the glass phase indicates that dissolution of Cs into the glass is preferred up to the solubility limit. The observation that the concentration of Cs dissolved in the glass phase of the Cs-CWF made with the 100CsCl:0NaCl salt was significantly higher than the concentration in the CWF made with the 50CsCl:50NaCl salt mixture indicates that the Cs concentration in the glass phase of the 50CsCl:50NaCl Cs-CWF was *not* solubility-limited. Considering that the glass contains more Na that can be exchanged, concentrations in the glass higher than 17 mass% Cs can probably be achieved by increasing the salt loading in the zeolite 4A beyond the 8 mass% used by Lambregts and Frank.

For the stoichiometric formation of sodalite by Reaction 1 and Cs-pollucite through Reaction 8, Cs accounts for 16.68 mass% of the crystalline phases. It is expected that the crystalline phases will occupy about 80 vol% of the waste form and the glass phase will occupy about 20 vol%. (As mentioned earlier, this will require using more than 20 mass% binder glass in the batched mixture because some glass will be consumed to provide SiO_2.) The maximum salt loading is predicted to be about 17 mass%. Higher loadings are expected to result in significant amounts of salt inclusions within the glass phase likely to be detrimental to waste disposal packages. However, as in the CWF made with surrogate 300 driver salt, salt inclusions of several mass% can probably be tolerated in waste forms made with Cs-rich salts.

Whereas the loading of EBR-II surrogate salt is determined primarily by the capacity of sodalite to sequester Cl^-, the loading of CsCl may also be affected by the availability of silica to produce Cs-pollucite and a glass composition that remains fluid enough to encapsulate the crystalline phases. In the Cs-CWF materials made by Lambregts and Frank (2002), the silica was provided by the glass, but the amount of glass that remained in the resulting Cs-CWF was not sufficient to encapsulate the other phases. This might be remedied by using a glass with a higher Na_2O content. Comparing the stoichiometries in Reactions 1 and 6, the waste loading of CsCl will be 33% lower than that of NaCl on a molar basis, but about 2-times higher on a mass basis. Increasing the Cs content of the waste salt will lower the waste loading on a mole basis, but remain similar to that achievable with EBR-II salt on a mass basis.

2.3 Mineral Phases and Waste Loading for FCRD Reference Salt

The possible encapsulation of the waste salts remaining after various processing operations in a glass-bonded mineral waste form is being evaluated based on previous experiments and analyses conducted during the development of the glass-bonded sodalite waste form for salt generated during treatment of spent sodium-bonded nuclear fuel, salt treatment (Simpson and Battisti 1999, Simpson 2003), and other mineralization approaches (e.g., Strachan and Badad 1979, Vance et al. 1982). Besides Cs, actual salt wastes will contain Rb, Sr, and Ba that will affect the phase composition of the ACWF. For example, it is not known if Rb-pollucite will form or all of the Rb will dissolve into the glass

$$\text{Na-O-Si}\equiv\text{glass} + \text{RbCl} \rightarrow \text{Rb-O-Si}\equiv\text{glass} + \text{NaCl}. \qquad \text{Reaction 10}$$

Both Ba^{2+} and Sr^{2+} are expected to dissolve into the glass to some extent by exchanging with two Na^{+} ions as

$$2\ \text{glass}{\equiv}\text{SiO-Na} + BaCl_2 \leftrightarrows \text{glass}{\equiv}\text{SiO-Ba-OSi}{\equiv}\text{glass} + 2\ NaCl \qquad \text{Reaction 11}$$

and

$$2\ \text{glass}{\equiv}\text{SiO-Na} + SrCl_2 \leftrightarrows \text{glass}{\equiv}\text{SiO-Sr-OSi}{\equiv}\text{glass} + 2\ NaCl. \qquad \text{Reaction 12}$$

It is also expected that celsian and stronsiocelsian will form by the reaction of some of the $BaCl_2$ and $SrCl_2$ with zeolite 4A as

$$\underset{\text{zeolite 4A}}{2\ Na_{12}(AlSiO_4)_{12}} + 3\ BaCl_2 \rightarrow \underset{\text{sodalite}}{3\ Na_8(AlSiO_4)_6Cl_2} + \underset{\text{celsian}}{3\ BaAl_2Si_2O_8} \qquad \text{Reaction 13}$$

and

$$\underset{\text{zeolite 4A}}{2\ Na_{12}(AlSiO_4)_{12}} + 3\ SrCl_2 \rightarrow \underset{\text{sodalite}}{3\ Na_8(AlSiO_4)_6Cl_2} + \underset{\text{stronsiocelsian}}{3\ SrAl_2Si_2O_8} \qquad \text{Reaction 14}$$

although this remains to be demonstrated. Note that these reactions do not consume silica.

The phases that form in the CWF products will depend on the relative rates of competing reactions and stabilities of the products. The exchange of Sr^{2+}, Ba^{2+}, Cs^{+}, and Rb^{+} (some or all) from the salt for Na^{+} from the glass by exchange will promote the formation of sodalite and consumption of zeolite 4A by increasing the Na concentration. If all the Rb^{+}, Sr^{2+}, and Ba^{2+} exchange with the glass to release Na^{+}, then the resulting salt composition will be similar to the 25CsCl:75NaCl mixture prepared by Lambregts and Frank (2002, 2003). Almost all of the Cs in that mixture appeared to enter the glass phase of that Cs-CWF product, and only trace amounts of Cs-pollucite were detected. If $SrCl_2$ reacts to form stronsiocelsian faster than NaCl reacts to form sodalite, for example, then less zeolite 4A will be available to form sodalite or Cs-pollucite. This would affect the distribution of Cs and other radionuclides.

A theoretical maximum waste loading can be calculated by using the stoichiometries of the mineral phases sequestering Na, Li, K, Rb, Cs, Ba, and Sr and the reactions to form them. Reactions 15 – 22 give the reactions to form minerals by reaction between zeolite 4A and the salt. Reactions to form pollucite and related minerals require added SiO_2, which is assumed to be provided by the glass. Based on the stoichiometries of the reactions to form these mineral phases, the masses of reagents required and products formed on a grams mineral-per-gram component salt basis are:

$$\underset{7.29}{Na_{12}(AlSiO_4)_{12}} + \underset{1}{4\ NaCl} \rightarrow \underset{8.29}{2\ Na_8(AlSiO_4)_6Cl_2} \qquad \text{Reaction 15}$$

$$\underset{0.357}{12\ SiO_2} + \underset{3.38}{4\ Na_{12}(AlSiO_4)_{12}} + \underset{1}{12\ LiCl} \rightarrow \underset{2.88}{6\ Na_8(AlSiO_4)_6Cl_2} + \underset{1.08}{12\ LiAlSi_2O_6} \qquad \text{Reaction 16}$$

$$\underset{0.357}{12\ SiO_2} + \underset{3.38}{4\ Na_{12}(AlSiO_4)_{12}} + \underset{1}{12\ KCl} \rightarrow \underset{2.88}{6\ Na_8(AlSiO_4)_6Cl_2} + \underset{1.50}{12\ KAlSi_2O_6} \qquad \text{Reaction 17}$$

$$\underset{0.497}{12\ SiO_2} + \underset{4.70}{4\ Na_{12}(AlSiO_4)_{12}} + \underset{1}{12\ RbCl} \rightarrow \underset{2.88}{6\ Na_8(AlSiO_4)_6Cl_2} + \underset{2.19}{12\ RbAlSi_2O_6} \qquad \text{Reaction 18}$$

$$\underset{0.357}{12\ SiO_2} + \underset{3.38}{4\ Na_{12}(AlSiO_4)_{12}} + \underset{1}{12\ CsCl} \rightarrow \underset{2.88}{6\ Na_8(AlSiO_4)_6Cl_2} + \underset{1.85}{12\ CsAlSi_2O_6} \qquad \text{Reaction 19}$$

$$\underset{0.357}{12\ SiO_2} + \underset{3.38}{4\ Na_{12}(AlSiO_4)_{12}} + \underset{1}{12\ CsI} \rightarrow \underset{2.88}{6\ Na_8(AlSiO_4)_6I_2} + \underset{1.85}{12\ CsAlSi_2O_6} \qquad \text{Reaction 20}$$

$$\underset{5.46}{2\ Na_{12}(AlSiO_4)_{12}} + \underset{1}{3\ BaCl_2} \rightarrow \underset{4.65}{3\ Na_8(AlSiO_4)_6Cl_2} + \underset{1.80}{3\ BaAl_2Si_2O_8} \qquad \text{Reaction 21}$$

$$\underset{7.17}{2\ Na_{12}(AlSiO_4)_{12}} + \underset{1}{3\ SrCl_2} \rightarrow \underset{6.11}{3\ Na_8(AlSiO_4)_6Cl_2} + \underset{2.05}{3\ SrAl_2Si_2O_8} \qquad \text{Reaction 22}$$

The values given under each reactant or product is number of grams for reaction with 1 g salt. The waste loading of each component was calculated as the mass of the salt component (which is 1.00 for each reaction) divided by the total mass of the products. Expressed as the mass%, the values for accommodating each of the cations in the waste salt in these product phases are 12.1% NaCl, 21.1% CsCl, 18.9% CsI, 16.1% RbCl, 15.5% $BaCl_2$, and 12.2% $SrCl_2$. These represent the maximum possible mass waste loading of each salt component **with no glass phase**, except for the SiO_2 that is a reactant to produce some phases. We emphasize that these are mass%. Even though appreciable amounts of Na, Cs, Rb, Ba, and Sr will dissolve into the glass, including the glass phase to encapsulate these phases will lower the waste loading by 25% or more.

Although large fractions of the Li^+ and K^+ in the LiCl/KCl salt will likely dissolve in the glass, upper bounds to the waste loadings of LiCl and KCl are estimated by assuming they form the Li and K analogues of pollucite. The maximum possible loading of the waste salt composition after the removal of lanthanides and actinides as given in Table 1 was estimated to be 21.8 mass% by multiplying the mass fraction of each element by the maximum loading of that element into the pollucite or celsian phase. If 25 mass % glass is required to (1) facilitate the reaction of salt, zeolite 4A, and SiO_2 from the glass to form the mineral phases and (2) bind the minerals into a mechanically stable waste form, then the maximum salt waste loading will be about 16.4 mass%. If more glass must be added to fully encapsulate these phases, the maximum salt waste loading will decrease proportionally.

3. ACWF PRODUCTION AND CHARACTERIZATION

A collaborative study with activities at ANL, INL, and PNNL is in progress to demonstrate that durable "advanced' CWF products can be made with ER salt waste at loadings of 12 mass% or higher (Ebert and Snyder 2015). The hypothesis being evaluated is that the binder glass used to make CWF materials can (1) provide some or all of the Na^+ needed to react with all the Cl^- in the waste salt to generate sodalite and a small amount of halite, and (2) accommodate most of the other cations from the waste salt within the resulting glass phase. This approach is being evaluated by producing and testing CWF materials made using several different glass compositions and various salt waste loadings. The experimental approach is being conducted in four phases:

- Phase 1 is a proof-of-concept study to demonstrate Na^+ can be provided by the glass to achieve high salt loadings. Five trial binder glasses with about 20 mass% Na_2O were formulated and made at PNNL. Prototype ACWF products formulated with 11 mass% loadings of a surrogate waste salt representing contaminated ER salt were made at INL for testing and analysis. The materials were characterized in detail at PNNL and subjected to corrosion tests at ANL to evaluate the degradation behavior and waste form performance.

- The focus of Phase 2 is to determine the limiting salt loading in ACWF materials made using one of the binder glasses evaluated in the Phase 1 study and determine aspects of the processing method that could improve the physical properties of ACWF materials, such as the efficiency of encapsulation and densification.

- In Phase 3, an improved binder glass composition was to be formulated by utilizing insights gained in the Phase 1 and Phase 2 activities and used to make new ACWF materials for testing.

- Phase 4 will demonstrate the flexibility of the ACWF to accommodate extreme salt waste compositions that may occur during waste decontamination operations for salt recycle, such as waste salts with high Li, Cs, or Sr concentrations.

At the time of writing, Phases 1 and 2 are almost completed and those results are being evaluated to determine the need to further modify the binder glass composition in Phase 3 and begin formulating ACWF materials for other salt compositions. The results for activities in Phases 1 and 2 are summarized in this section and Section 4.

3.1 Waste Form Production

3.1.1 Salt

Table 3 summarizes salt compositions that have been used to represent the nominal waste salts from fuel processed using the eutectic LiCl/KCl salt in recent studies. The EBR-II salt composition represents waste salt generated after processing 300 spent sodium-bonded driver fuel assemblies that were irradiated to high burn-up and enriched in ^{235}U. This was the nominal composition used in the CWF formulations for disposing salt without recycle and is referred to as "300 driver salt" (Ebert 2005). The Bateman salt composition represents a simplification of the EBR-II salt that was used for full-scale demonstrations at INL (Bateman et al. 2007). The Vienna salt composition represents the average of several estimated compositions based on different recycling efficiencies (Vienna 2015).

Table 3. Simulated waste salt compositions, in mass %

	EBR-II	Bateman	Vienna	ER salt
LiCl	31.4	31.1	33.9	33
KCl	38.4	37.8	43.1	41
NaCl	14.9	15	11.3	10
CsCl	2.51	3	2.3	3
KI	0.15	0.2	—	3
$RbCl_2$	0.33	—	—	—
$SrCl_2$	1.00	2.2	2.5	3
$BaCl_2$	1.20	—	—	—
$SmCl_2$	0.69	—	—	—
$EuCl_2$	0.05	—	—	—
$CeCl_3$	2.33	5	1.8	2
YCl_3	0.70	0.2	—	—
$LaCl_3$	1.22	—	—	—
$PrCl_3$	1.15	—	—	—
$NdCl_3$	3.90	5	5.1	5

The ER salt composition is the target for the salt used to make ACWF products for testing in the MRWFD activities. It is a simplification of the Vienna salt composition, except slightly higher Cs, Sr, and I contents are used to facilitate tracking the disposition and release behaviors of those elements. The higher concentrations of these elements were balanced by using a slightly lower NaCl concentration. Table 4 provides the targeted and measured elemental composition of the large batch of ER salt that was prepared to make the ACWF products for these testing activities.

Table 4. ER salt composition, elemental mass fraction

Element	As-batched	Measured	Element	As-batched	Measured
Li	0.0525	0.0530	Sr	0.0166	0.0169
K	0.2210	0.2150	Y	0.0066	0.0069
Na	0.0437	0.0380	La	0.0088	0.0086
Cs	0.0397	0.0400	Nd	0.0117	0.0113
I	0.0228	0.0231	Cl^-	0.5766	0.5872

3.1.2 Zeolite 4A

The zeolite 4A was prepared in the same way to make all CWF and ACWF materials (see Appendix A, Table A.2), except the zeolite 4A used was ground with a mortar and pestle to produce the -200 mesh size fraction used to make ACWF-N4F-11. The zeolite 4A composition is given in Table 5. It was dried to the same low water content before salt occlusion (<1 mass% water).

Table 5. Zeolite 4A composition, elemental mass fraction

Element	Si	Al	Na	O
f(i)	0.1977	0.1899	0.1618	0.1505

3.1.3 Binder Glass

The CWF materials are referred to as being "advanced" because the binder glass used to produce them was formulated with higher Na_2O contents to support higher salt waste loadings. The compositions of binder glasses used to make CWF and ACWF materials are summarized in Table 6. The P57 glass used to develop the CWF was selected based on empirical evaluations of whether or not an acceptable material could be produced using materials made by using a wide range of glass compositions, including bottle glasses and glasses specially formulated for use as waste forms. This was done by trial and error. Corning glass C7056 was used to make CWF materials for demonstration purposes after P57 glass became commercially unavailable in the early 2000s.

The series of sodium borosilicate (NBS) glasses that are referred to as NBS-2, NBS-3, NBS-4, NBS-5, and NBS-6 was formulated and made with the objective of designing a binder glass with a higher Na_2O content to produce ACWF materials with higher salt waste loadings. All the NBS glasses have about 3-times the Na_2O content of P57 and C7056 has about one-third. The NBS glasses were formulated to match physical properties of P57 glass that could affect encapsulation of sodalite and the acceptability of the resulting ACWF products; properties of P57 and the NBS series glasses are included in Table 6.

Table 6. Glass compositions, elemental mass fraction

f(i)	P57	C7056	NBS-2	NBS-3	NBS-4	NBS-5	NBS-6
Si	0.3108	0.3281	0.2798	0.2752	0.2752	0.2379	0.2296
B	0.0593	0.0677	0.0310	0.0279	0.0279	0.0511	0.0585
Al	0.0360	0.0132	0.0264	0.0475	0.0317	0.0475	0.0459
Ca	—	—	—	—	0.0285	—	—
Na	0.0527	0.0171	0.1497	0.1497	0.1497	0.1497	0.1484
Zr	0.0000	0.0000	0.0369	0.0222	0.0148	0.0259	0.0250
K	0.0042	0.0266	—	—	—	—	—
O	0.5370	0.5473	0.4762	0.4776	0.4723	0.4880	0.4927
Al/Si	0.12	0.04	0.09	0.17	0.12	0.20	0.20
ρ, g cm^{-3}	2.269	—	2.559	2.485	2.525	2.489	2.300
T_M, ℃	1550	—	1550	1550	1550	1450	1350
T_G, ℃	516	—	560	554	543	552	545
T_s, ℃	570	—	608	594	583	590	582

3.1.4 CWF and ACWF Production

The gross compositions of the ACWF materials were calculated based on the compositions and relative amounts of salt, zeolite 4A, and binder glass used to produce them. These are summarized in Table 7. The effect of the glass composition on waste form durability was evaluated further by conducting tests with two CWF products that had been made previously using P57 glass and Corning 7056 glass and 8 mass% salt. These are referred to as CWF-P5-8 and CWF-C1-8. The Corning 7056 glass was used in the last of the four full- scale surrogate waste forms made to demonstrate the PC production method (Bateman et al. 2007). As was shown in Table 3, the compositions of the salts used to make these two CWF materials differed slightly from that of the salt used to make the ACWF materials.

Although P57 glass is no longer commercially available, a small amount of P57 glass remains available at INL for use in laboratory-scale testing. Two CWF products were made with P57 glass to show the effect of the glass composition on the production and performance of the final waste form by direct comparison

Table 7. Formulations and CWF and ACWF compositions, mass fraction

Material ID:	CWF-C1-8	CWF-P5-8	CWF-P1-8	CWF-P6-11	ACWF-N2-11	ACWF-N3-11
Salt ID[a]	Bateman	EBR-II	EBR-II	EBR-II	ER	ER
Salt	0.080	0.080	0.078	0.110	0.110	0.110
Zeolite 4A	0.670	0.670	0.401	0.629	0.629	0.629
Glass ID[b]	C7056	P57	P57	P57	NBS-2	NBS-3
Glass	0.250	0.250	0.520	0.260	0.260	0.260
Si	0.2145	0.2102	0.2411	0.2053	0.1973	0.1961
B	0.0169	0.0148	0.0309	0.0154	0.0081	0.0073
Al	0.1306	0.1362	0.0949	0.1289	0.1264	0.1319
Ca	—	—	—	—	—	—
Na	0.1162	0.1251	0.0958	0.1204	0.1456	0.1456
Zr	0.0000	0.0000	0.0000	0.0000	0.0096	0.0058
K	0.0243	0.0187	0.0195	0.0255	0.0244	0.0244
O	0.4387	0.4361	0.4602	0.4233	0.4075	0.4078
Li	0.0042	0.0042	0.0041	0.0058	0.0058	0.0058
Cs	0.0032	0.0032	0.0031	0.0044	0.0044	0.0044
I	0.0018	0.0018	0.0018	0.0025	0.0025	0.0025
Sr	0.0013	0.0013	0.0013	0.0018	0.0018	0.0018
Y	0.0005	0.0005	0.0005	0.0007	0.0007	0.0007
La	0.0007	0.0007	0.0007	0.0010	0.0010	0.0010
Nd	0.0009	0.0009	0.0009	0.0013	0.0013	0.0013
Cl^-	0.0461	0.0461	0.0452	0.0637	0.0637	0.0637

Material ID:	ACWF-N4-11	ACWF-N5-11	ACWF-N4-12	ACWF-N4-14	ACWF-N6-11	ACWF-N4G-10
Salt ID	ER	ER	ER	ER	ER	ER
Salt	0.110	0.110	0.120	0.140	0.110	0.100
Zeolite 4A	0.629	0.629	0.667	0.700	0.629	0.500
Glass ID	NBS-4	NBS-5	NBS-4	NBS-4	NBS-6	NBS-4
Glass	0.260	0.260	0.213	0.160	0.260	0.400
Si	0.1961	0.1863	0.1905	0.1824	0.1842	0.2089
B	0.0073	0.0133	0.0059	0.0045	0.0152	0.0112
Al	0.1278	0.1319	0.1334	0.1380	0.1319	0.1076
Ca	0.0074	—	0.0061	0.0046	—	0.0114
Na	0.1456	0.1456	0.1451	0.1434	0.1453	0.1452
Zr	0.0038	0.0067	0.0032	0.0024	0.0065	0.0059
K	0.0244	0.0244	0.0265	0.0309	0.0244	0.0221
O	0.4065	0.4105	0.4011	0.3909	0.4118	0.4142
Li	0.0058	0.0058	0.0063	0.0074	0.0058	0.0053
Cs	0.0044	0.0044	0.0048	0.0056	0.0044	0.0040
I	0.0025	0.0025	0.0027	0.0032	0.0025	0.0023
Sr	0.0018	0.0018	0.0020	0.0023	0.0018	0.0017
Y	0.0007	0.0007	0.0008	0.0009	0.0007	0.0007
La	0.0010	0.0010	0.0011	0.0012	0.0010	0.0009
Nd	0.0013	0.0013	0.0014	0.0016	0.0013	0.0012
Cl^-	0.0637	0.0637	0.0692	0.0807	0.0637	0.0577

[a]See Table 3.
[b]See Table 6.

with the ACWF: CWF-P1-8 was made with the amount of P57 glass require to provide the same amount of Na that is provided by the NBS glasses and CWF-P6-11 was made with 11 mass% salt loading to evaluate the effect of the Na content in the glass products. The as-batched amount of salt, zeolite 4A, and binder glass used to make the CWF and ACWF products for testing and analyses and the processing conditions are summarized in Table 8. (See Appendix A Sections A.1-A.5) for details on processing.

Table 8. Material preparation details

Product ID	Salt mass, g	Zeolite 4A mass, g	Salt loading, mass %	SLZ mass, g	Glass ID	Glass mass, g	Time at 925 ℃, h
			Archived Materials				
CWF-P5-8	8.34	69.38	8	77.69	P57	25.90	16
CWF-C1-8	28400	255400	8	283800	C7056	94600	36
			Phase 1 Materials				
CWF-P1-8	3.9209	20.0718	8	23.7235	P57	25.6321	16
CWF-P6-11	11.4632	65.1044	11	36.9340	P57	13.0200	5
ACWF-N2-11	11.4632	65.1044	11	36.9751	NBS-2	13.0314	16
ACWF-N3-11	11.4632	65.1044	11	36.9799	NBS-3	13.0272	16
ACWF-N4-11	11.3903	65.0659	11	36.9879	NBS-4	13.0302	16
ACWF-N5-11	11.3903	65.0659	11	36.9853	NBS-5	13.0223	16
ACWF-N6-11	5.5353	31.4662	11	37.0015	NBS-4	12.9073	24
			Phase 2 Materials				
ACWF-N4F-11[a]	5.5223	31.4706	11	36.9929	NBS-4	13.0122	24
ACWF-N4-12	5.9980	30.9714	12	36.9694	NBS-4	13.0353	24
ACWF-N4-14	7.0076	29.9882	14	36.9959	NBS-4	13.0846	24
ACWF-N4G-10	TBD	TBD	10	TBD	TBD	TBD	TBD

[a]N4F indicates material made with -200 mesh zeolite 4A and -200 mesh glass.

The first set of CWF and ACWF products was made for Phase 1 testing by using P57 and the new binder glasses formulated and made with the primary objective of selecting one glass composition for further development and use in Phase 2 testing. The ACWF products were made in FY 2015 using each binder glass with 11 mass% loading of the ER salt to compare the effectiveness of each glass in generating sodalite with only small amounts of halite. An amount of salt less than the theoretical maximum salt loading was used in this initial series so that the performance of the binder glass could be distinguished from of the completion of the reactions to form sodalite. The primary objective of the initial study was to prove the concept and justify the approach for increasing the salt waste loadings by using a binder glass with a higher Na_2O content. Photographs of the first set of CWF and ACWF products are shown in Figure 3. The ACWF products made using the various binder glasses are identified by the glass binder that was used and salt waste loading. For example, ACWF-N4-11 was made using NBS-4 glass with 11 mass% waste salt loading.

A second set of ACWF materials was made in FY 2016 using the binder glass NBS-4 with 12% and 14% loadings of the ER salt. These represent salt loadings at near the theoretical maximum to evaluate the impact of the salt content on waste form production and performance. Two additional materials were made to evaluate approaches to decrease the porosity of the ACWF products: ACWF-N4F-11 was made with 11% salt loading using crushed zeolite 4A and crushed NBS-4 glass (both were sized to -200 mesh,

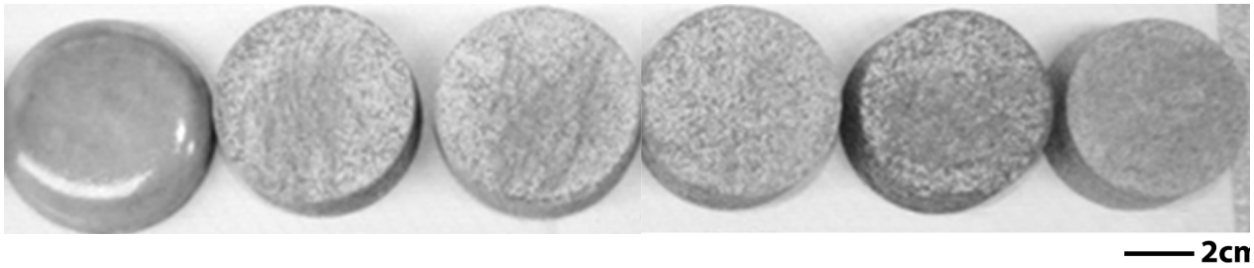

Figure 3. Photographs of (left to right): Phase 1 products CWF-P1-8, ACWF-N2-11, ACWF-N3-11, ACWF-N4-11, ACWF-N5-11, and CWF-P6-11.

which is <75 µm) and ACWF-N4G-10 made with 10% salt loading by increasing the amount of NBS-4 glass in the mixture. The formulation and composition of ACWF-N4F-11 are identical to that of ACWF-N4-11, which was made with the standard size fraction of zeolite 4A. The formulation and composition ACWF-N4G-10 are based on ACWF-N4-14 with extra glass added to attain 40 mass% glass in the final product. Another Phase 1 product ACWF-N6-11 was made using NBS-6 glass that was formulated with a higher B content than the other new binder glass. Photographs of the second set of products are shown in Figure 4. Tests and analyses with ACWF-N6-11 and ACWF-N4G-10 have not yet been completed.

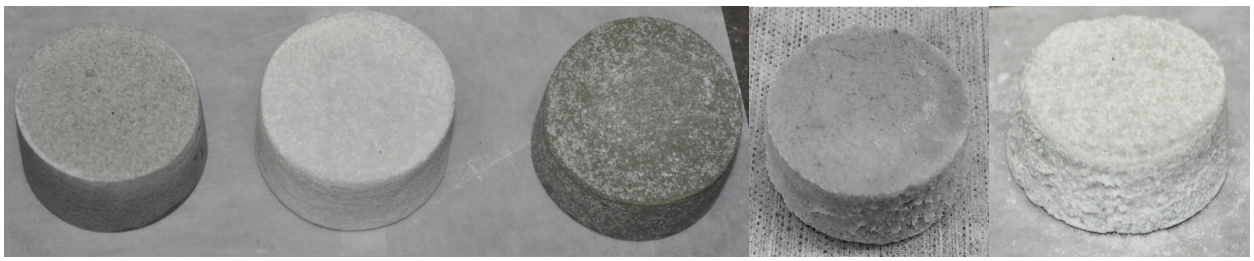

Figure 4. Photographs of (left to right): Phase 2 products ACWF-N4F-11, ACWF-N4-12, ACWF-N4-14, ACWF-N4G-10, and Phase 1 product ACWF-N6-11.

3.2 Characterization of CWF and ACWF Products

3.2.1 Physical and Chemical Characterization

The CWF and ACWF products were cut into pieces that were used for characterization and as test specimens. All materials were cut and polished using absolute ethanol as a cutting fluid to minimize dissolution of any residual salt and halite inclusions. All materials were visibly porous except CWF-P1-8, which was made with a high glass content. Photomicrographs of three materials by optical microscopy are shown in Figure 5. The porosities of ACWF-N4-11 and ACWF-N4-14 are representative of most materials. The porosity of ACWF-N4F-11, which was made with finely crushed zeolite 4A in an effort to increase the density, appeared to be much lower with the unaided eye and under the optical microscope at low and intermediate magnifications. However, the total porosities of materials made with standard and size-reduced zeolite 4A appear to be similar under high magnification.

Pieces cut from each CWF and ACWF product were used to measure the density and open porosity by using the Archimedes method. Details of the analyses are provided in Appendix A Section A.6. Results

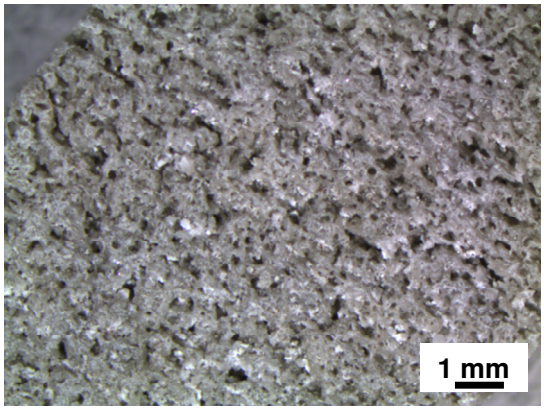

(a) ACWF-N4-11 at low magnification

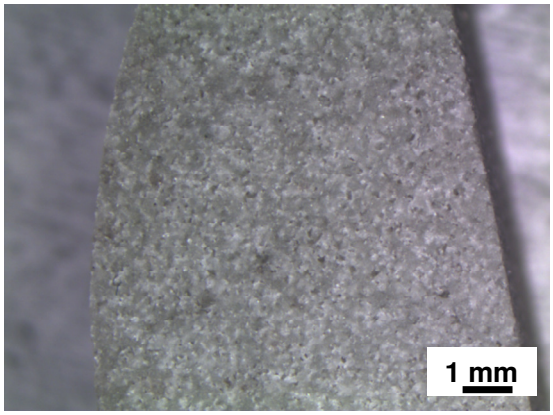

ACWF-N4F-11 at low magnification

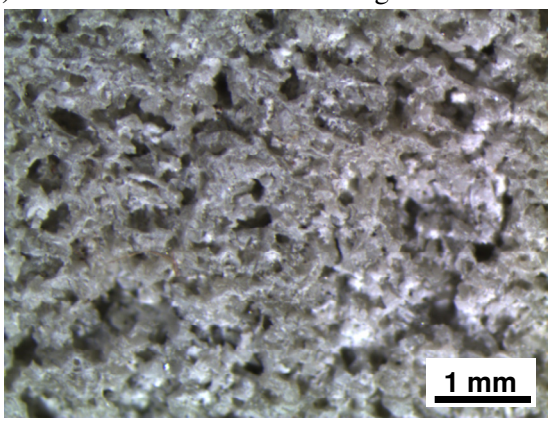

(b) ACWF-N4-11 at intermediate magnification

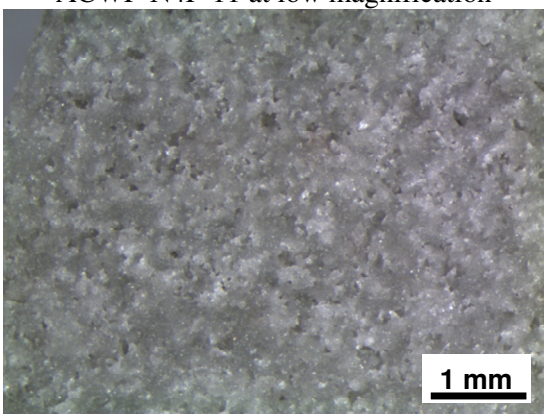

ACWF-N4F-11 at intermediate magnification

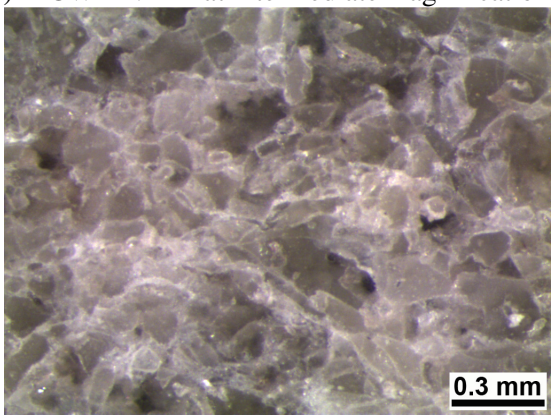

(c) ACWF-N4-14 at high magnification

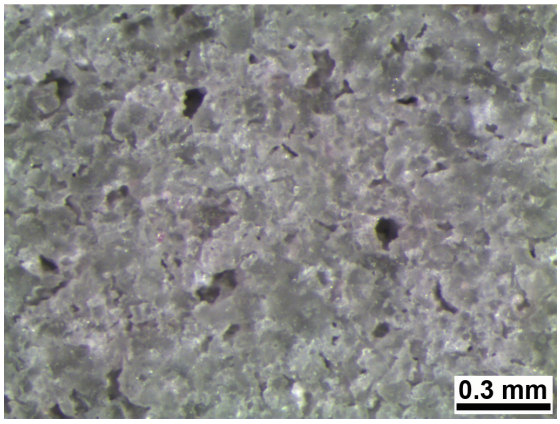

ACWF-N4F-11 at high magnification

Figure 5. Optical photomicrographs of ACWF-N4-11 and ACWF-N4F-11 products at (a) low and (b) intermediate magnifications and (c) ACWF-N4-11 and ACWF-N4F-11 products at high magnification.

are summarized in Table 9. The CWF-P1-8 product was very dense, as expected considering the high glass loading, but the materials made with higher SLZ:glass loadings (74:26, by mass%) were all visibly porous. The measured porosity and density values are consistent with these observations. The area fractions of voids measured for polished cross sections of the different products by using SEM (see Section 3.2.2) are included for comparison. The volume and area fractions of voids are in good

Table 9. Measured phase composition, density, volumetric porosity, and surface porosity of CWF and ACWF products

Product ID	Phase Composition, mass %			Density, g cm^{-3}	Porosity, vol %	Porosity, area %
	Sodalite	NaCl	Glass			
Archived Materials						
CWF-P1-8	8.5	5.5	86	2.13	0.7	3.5
CWF-P6-11	39	4.2	57	1.50	33	43
Phase 1 Materials						
ACWF-N2-11	57	2.9	40	1.35	42	43
ACWF-N3-11	62	2.9	35	1.30	44	44
ACWF-N4-11	63	3.1	34	1.28	45	54
ACWF-N5-11	62	2.6	35	1.44	38	35
ACWF-N6-11	68	2.4	30	1.44	37	38
Phase 2 Materials						
ACWF-N4F-11	70	3.7	26	1.45	38	40
ACWF-N4-12	67	3.6	29	1.37	42	33
ACWF-N4-14	61	7.5	31	1.40	40	26
ACWF-N4G-10	TBD	TBD	TBD	TBD	TBD	TBD

agreement and similar for all ACWF materials. Samples of each material were pulverized to powders in a shatter box and used in powder x-ray diffraction (XRD) measurements (see Section 3.2.4); the phase compositions are included in Table 9.

The chemical compositions of three ACWF products were measured to verify material was not lost during production and justify use of the as-batched compositions. Small pieces of ACWF-N3-11, ACWF-N4-12, and ACWF-N4-14 were chemically dissolved and analyzed by inductively-coupled mass spectrometry (ICP-MS) and chloride ion selective electrode to verify there were not significant mass losses during production. The compositions that were calculated from the as-batched composition and measured analytically are given in Table 10. These results confirm the increasing concentrations of salt constituents.

Table 10. Measured compositions of ACWF-N3-11, ACWF-N4-12, and ACWF N4-14, as mass fraction

	ACWF-N3-11		ACWF-N4-12		ACWF-N4-14	
Element	Calculated	Measured	Calculated	Measured	Calculated	Measured
Si	0.1961	0.195	0.1905	0.1939	0.1824	0.2011
B	0.0073	0.0066	0.0059	0.0065	0.0045	0.0067
Al	0.1319	0.112	0.1334	0.1403	0.1380	0.1447
Ca	0	—	0.0061	NA	0.0046	NA
Na	0.1456	0.141	0.1451	0.1192	0.1434	0.1253
Zr	0.0058	0.0055	0.0032	0.0037	0.0024	0.0037
K	0.0244	0.0235	0.0265	0.1267	0.0309	0.0316
Li	0.0058	0.0054	0.0063	0.0061	0.0074	0.0075
Cs	0.0044	0.0037	0.0048	0.0039	0.0056	0.0052
I	0.0025	NA	0.0027	NA	0.0032	NA
Sr	0.0018	0.0017	0.0020	0.0021	0.0023	0.0024
Y	0.0007	0.0006	0.0008	0.0008	0.0009	0.0009
La	0.0010	0.0008	0.0011	0.0011	0.0012	0.0013
Nd	0.0013	0.0011	0.0014	0.0014	0.0016	0.0016
Cl^-	0.0637	0.0929	0.0692	0.0683	0.0807	0.0757

3.2.2 Scanning Electron Microscopy

Polished cross sections were prepared for SEM examinations by polishing in absolute ethanol or non-aqueous lubricant (see Appendix A Section A.7). Representative SEM photomicrographs of the materials made for Phase 1 are shown in Figures 6 and 7. Figure 6 provides relatively low magnification views of CWF-P6-8 and ACWF-N2-11 showing several sodalite regions encapsulated by glass. The edges of two large pores are seen in the photomicrograph of ACWF-N2-11 (black regions on the left and top of the photomicrograph are filled with resin used to prepare the cross section) and significant numbers of small pores are seen within the glass and sodalite regions. Fewer pores are evident in CWF-P6-8, but cracks are seen to penetrate glass and sodalite regions.

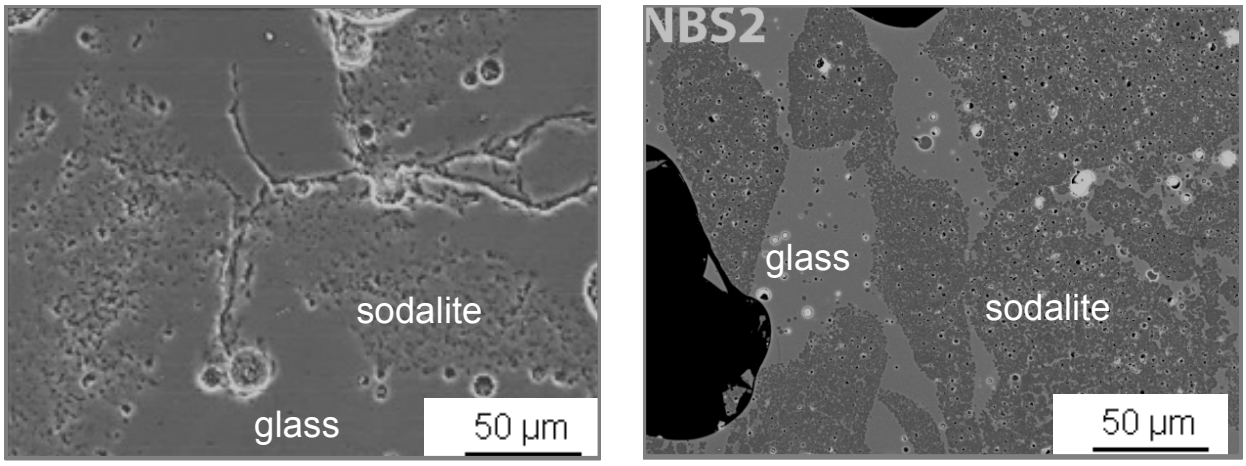

(a) (b)

Figure 6. SEM photomicrographs of (a) CWF-P6-8 and (b) ACWF-N2-11.

Photomicrographs of the sodalite/glass interfaces of the Phase 1 materials are shown at higher magnification in Figure 7. Glass is seen to have penetrated between the sodalite crystallites into the sodalite domains during processing. The sodalite domains in ACWF-N2-11, CWF-N3-11, CWF-N4-11, and CWF-N5-11 are apparent by distinct contrast differences where the sodalite domains are darker and the glass phase is notably brighter due to average atomic number contrast (lower *Z* is darker, higher *Z* is brighter). Although the sodalite-glass interface in CWF-P1-08 is difficult to identify based on contrast differences, the interface is clearly identified by the void spaces within the sodalite domains. The open porosity discussed previously was confirmed by the SEM analyses: CWF-P1-8, ACWF-N2-11, ACWF-N3-11, ACWF-N4-11, and ACWF- N5-11 were all quite porous; CWF-P1-8 did not contain any visible open porosity but did have many small bubbles (closed porosity). While the materials made with 11 mass% salt loading and 26 mass% binder glass were all fairly porous, it is likely the porosities would decrease somewhat with larger sample volumes and longer heat-treatment times, although higher temperatures would likely promote decomposition of sodalite into nepheline and halite. That may not be detrimental to the waste form durability.

The bulk elemental analyses of key components are shown in Figure 8 as EDS dot maps. The Cl^- has clearly been transferred from the salt and Na^+ has been transferred from the glass and incorporated in the sodalite phase. The resolution is not sufficient to unambiguously detect halite (NaCl) inclusions, and the bright spots in the Cl^- maps are probably artifacts, many of which appear to be associated with pores.

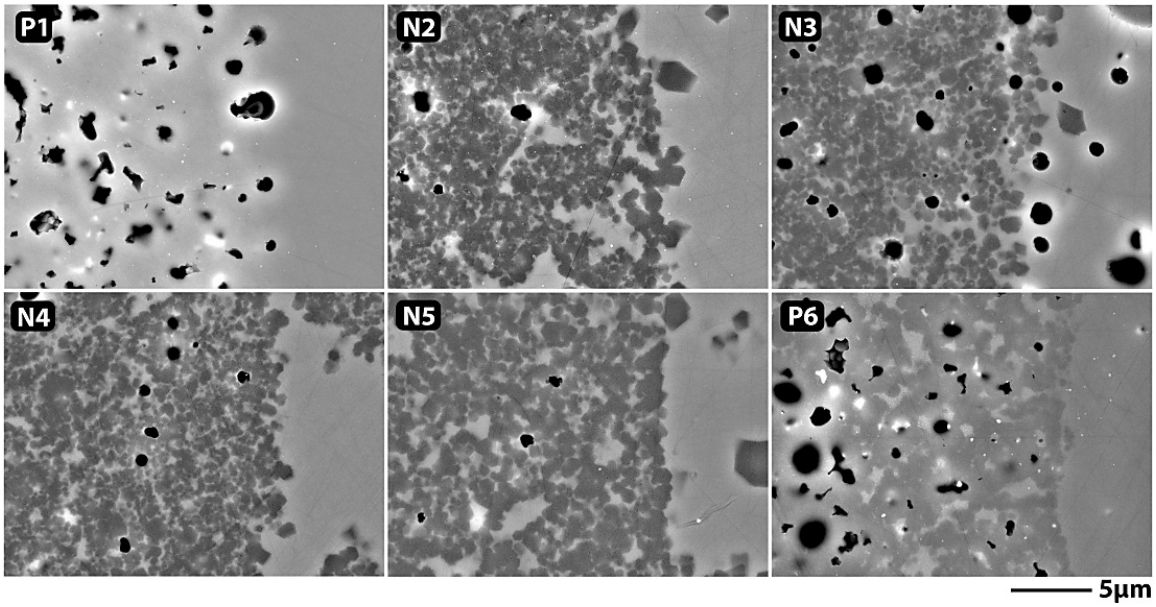

Figure 7. SEM photomicrographs of (top row left to right) CWF-P1-8, ACWF-N2-11, ACWF-N3-11, and (bottom row left to right) ACWF-N4-11, ACWF-N5-11, and CWF-P6-11 products.

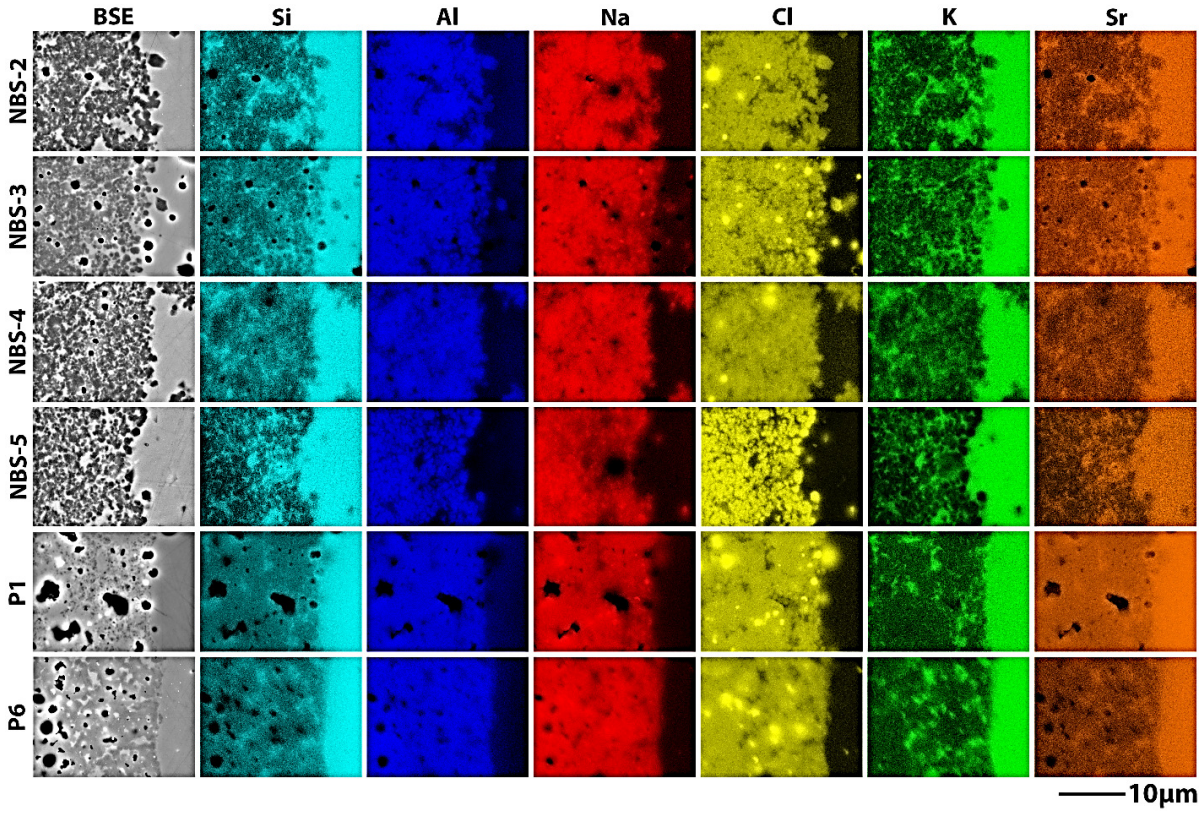

Figure 8. SEM photomicrographs and EDS elemental dot maps near sodalite/glass interfaces of (top to bottom) ACWF-N2-11, ACWF-N3-11, ACWF-N4-11, ACWF-N5-11, CWF-P1-8, and CWF-P6-11.

Both K^+ and Sr^{2+} have been transferred from the salt to the glass phases in all CWF and ACWF products. Note that the K and Sr detected within the sodalite domains are in glass that has penetrated between the sodalite grains, not in the sodalite. The Cs concentrations were below the detection limit, but Cs^+ is expected to be present in the glass phase based on the results of Lambregts and Frank discussed in Section 2.2. The Si content of the glass is much higher than the Si content of sodalite, but the Al content of sodalite is much higher than the Al content of the glass. The Al/Si mass ratios of the binder glasses based on the compositions given in Table 6 range from about 0.1 to about 0.2 for P57 and the NBS glasses, whereas the Al/Si mass ratio in sodalite is calculated to be about 0.96. The Al and Si contents in the CWF and ACWF materials are consistent with those in the reactants, and their (absolute) concentrations in the glass phase do not vary significantly during waste form production. Changes in the glass compositions due to waste form production are due to the exchange of Na^+ for other alkali and alkaline earth elements from the salt.

3.2.3 Secondary Ion Mass Spectrometry

Elemental mapping was also performed using secondary ion mass spectrometry (SIMS) to measure concentrations of B and Li across a sodalite-glass interface in ACWF-N3-11 (see Appendix A Section A.8). These area maps are shown in Figure 9. The concentrations of B and Li were found to be much higher in the glass phase than in sodalite, which indicates B remained in the glass and Li was transferred from the salt. Transfer of Na from the glass to the sodalite and K from the salt to the glass is also evident. Furthermore, the ToF-SIMS analysis indicates that an appreciable amount of Na remains in the glass phase. This is consistent with the expectation that 11% was below the maximum achievable salt loading in the ACWF materials. Base on the chemistry of reacting NaCl with zeolite 4A to produce sodalite, the 20% Na_2O content of NBS-3 and the other new binder glasses is sufficient to support the generation of enough sodalite to incorporate all the Cl^- in the salt, but the relative amount of glass used in the ACWF products is not sufficient to encapsulate that sodalite.

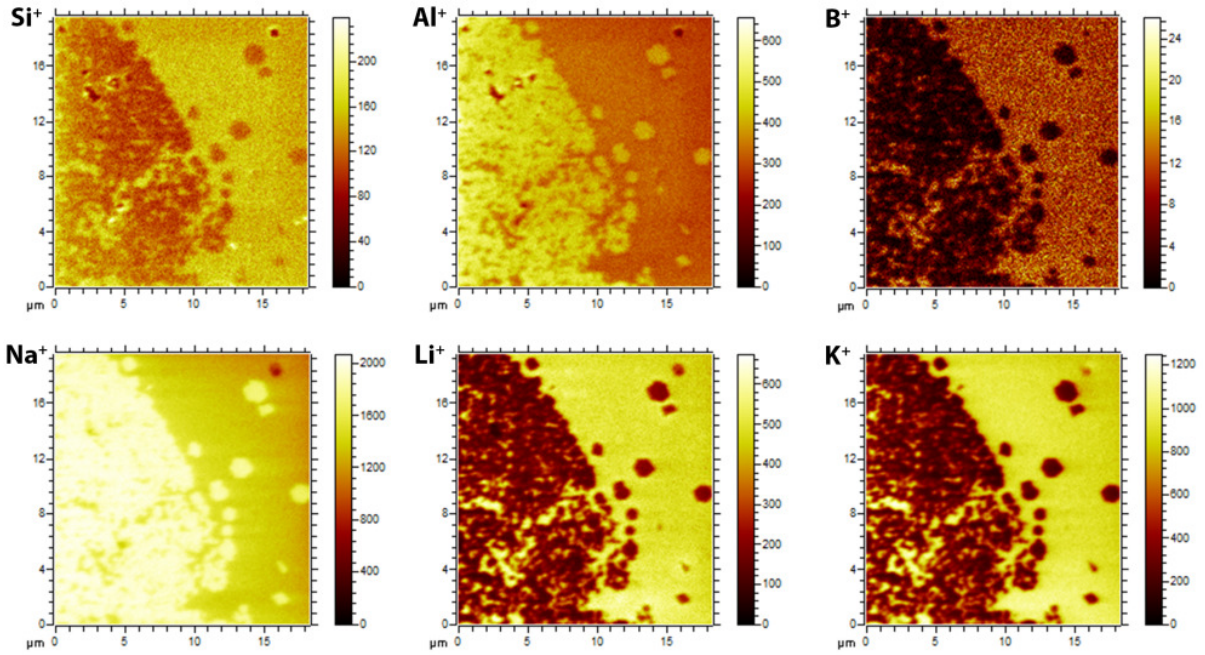

Figure 9. ToF-SIMS data for ACWF-N3-11 showing element distributions near a sodalite/glass interface.

3.2.4 Powder X-ray Diffraction

X-ray diffraction analyses showed sodalite was the dominant phase in all materials and halite was a minor phase in most materials (see Appendix A Section A.9). Representative spectra are shown in Figure 10 to indicate the close similarities for different CWF and ACWF products. The relative amounts of each phase determined by quantitative analysis with Rietveld refinements are included in Table 10. Small differences in the spectra are seen near the major halite peaks at about 31.7° and 45.4°. Additional scans made bracketing those peaks are shown in Figure 11 for ACWF-N3-11, ACWF- FN4-11, and ACWF-N4-14. The peaks at about 31.9° and 45.7° are from sodalite. The ratios of the neighboring halite and sodalite peaks are used to indicate the relative salt content. That the highest ratios of the 31.7°/31.9° peaks and the 45.4°/45.7° peaks are observed in the spectrum for the ACWF-N4-14 product (blue curves) indicates the halite content is likely greater at the highest salt loading. The sodalite peaks in both regions are almost identical for the ACWF-N3-11 and ACWF- FN4-11 products made with different binder glasses but the same salt waste loading. The finely crush zeolite 4A and glass used to make the ACWF- FN4-11 product did not have an obvious effect on the phase composition. Unidentified peaks at about 31.5° and 45.1° are present in the spectra for the two materials made with NBS-4 glass but not the spectrum for the material made with NBS-3 glass (black curves). The cause of these unidentified subtle differences is not known, but not expected to significantly impact waste form performance.

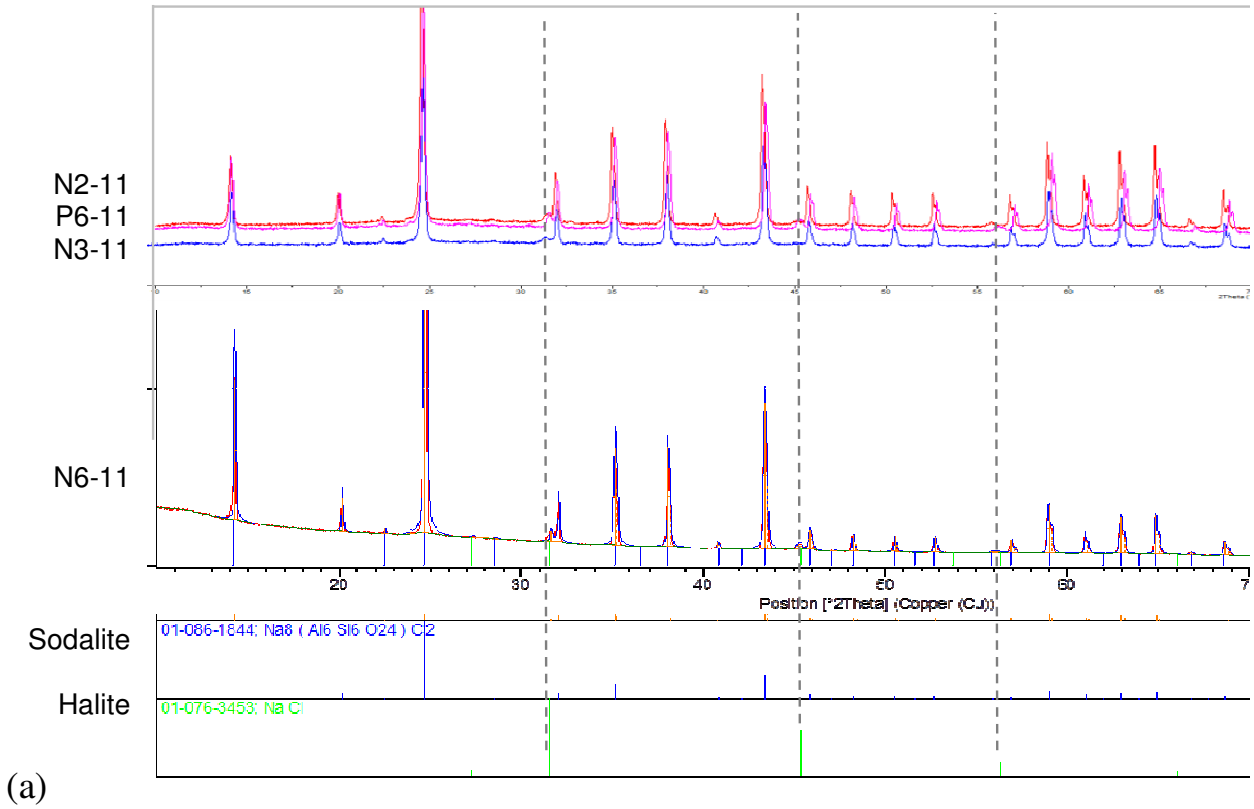

Figure 10. Compilations of XRD spectra for (a) ACWF-N2-11, CWF-P6-11, ACWF-N3-11, and ACWF-N6-11 and (b) ACWF-N4F-11, ACWF-N4-12, and ACWF-N4-14. Vertical dashed lines are included to facilitate comparisons of major halite peaks in the different materials.

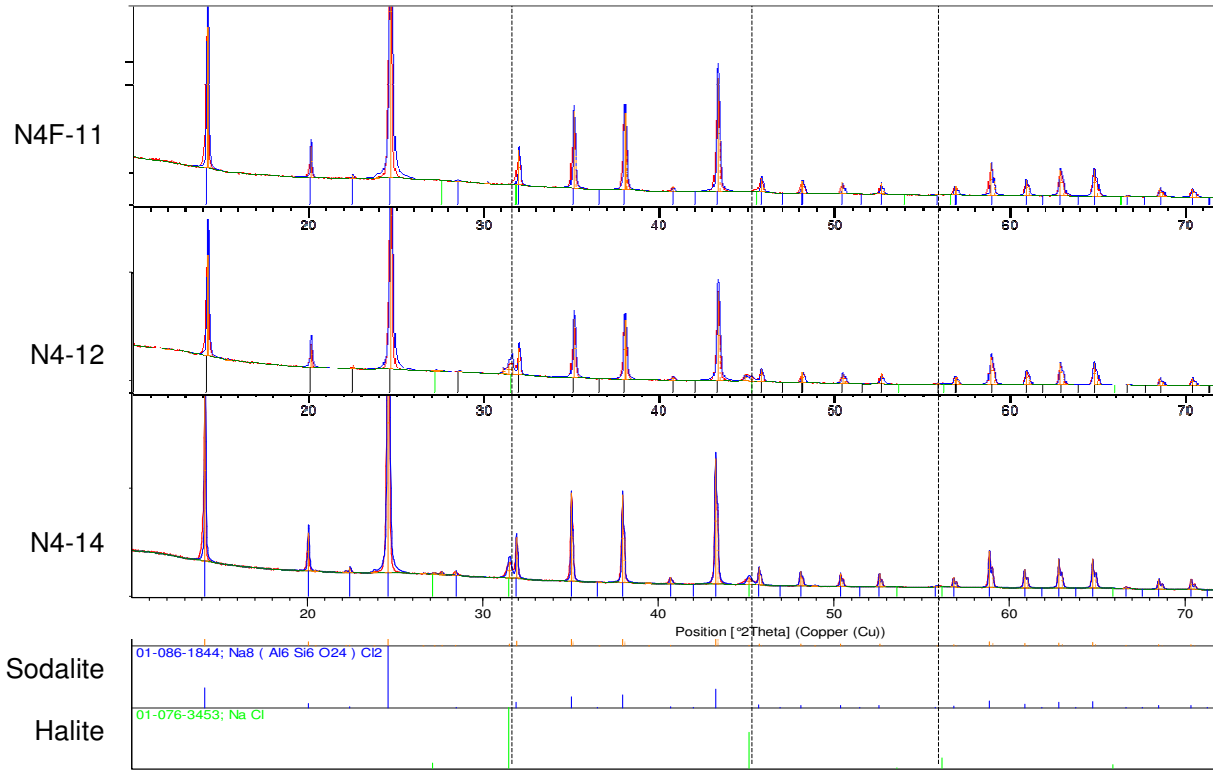

(b)

Figure 10. (cont.)

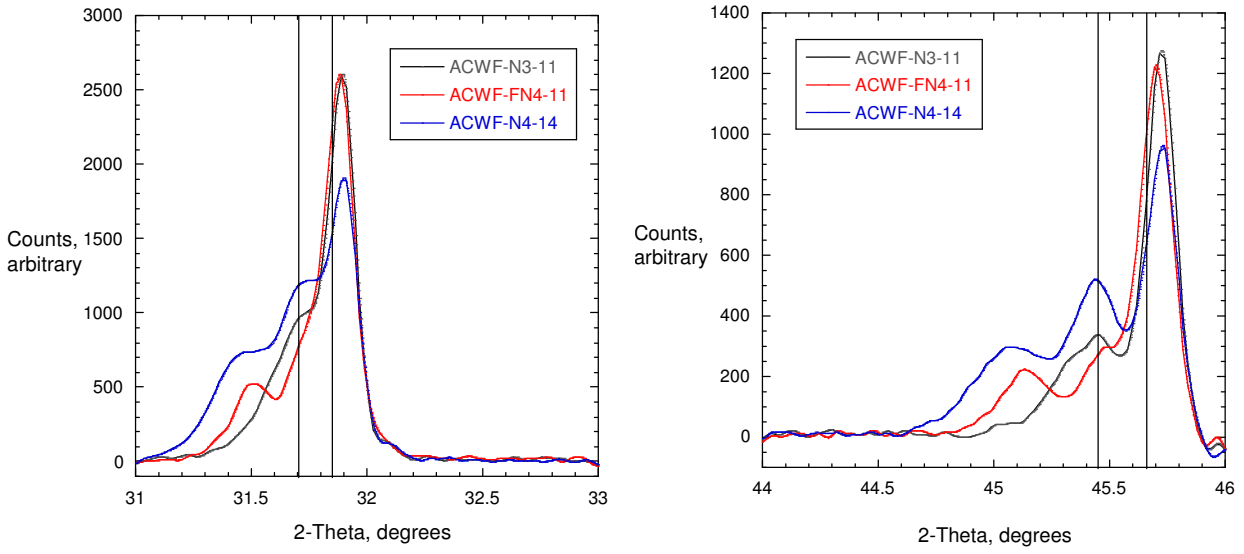

Figure 11. Two regions in XRD scans near major halite peaks for ACWF-N3-11 (black curves), ACWF- FN4-11 (red curves), and ACWF-N4-14 products (blue curves). Lines locate halite peaks at 31.705° and 45.45° and sodalite peaks at 31.85° and 45.66°.

4. CWF AND ACWF DEGRADATION TESTS

4.1 Degradation Test Methods

The degradation behaviors of CWF materials have been evaluated using a variety of test methods and the processes contributing are known and understood (Ebert 2005). Dissolution of the binder glass, sodalite, halite, and other inclusion phases occur simultaneously and essentially independently when contacted by water: halite dissolves instantaneously and has a very high solubility, sodalite dissolves at a moderate rate but has a low solubility, and the binder glass dissolves at a moderate rate and has a moderate solubility. All degrade by surface dissolution mechanisms. The chemical reaction affinities for sodalite and binder glass dissolution are coupled through a common dissolved silica concentration, but their very different solubilities make that a minor effect and they can be treated as if they dissolve independently. A strategy was developed to distinguish the dissolution of halite, sodalite, and the binder glass based on specific elements: B is only present in the binder glass, Cl^- is present in halite and sodalite, Si is present in sodalite and the binder glass, and Na is present in all three phases. The ratios of elemental solution concentrations can be compared with the stoichiometries of the phases to estimate the dissolution rates under test conditions that maintain conditions dilute enough that solution feedback effects can be ignored. This is demonstrated below.

Dissolution of the binder glass must occur before halite inclusions in the bulk can be dissolved. Glass dissolution is not significantly affected by the low silica concentration at which the solution becomes with saturated respect to sodalite. Sodalite and halite contain only small amounts of radionuclides and their dissolution only releases small amounts of radioiodide into solution; the majority of radionuclides are incorporated into the glass phase and only released as that dissolves. From the perspective of waste form performance, CWF degradation can be treated like HLW glass dissolution with the addition of a term for the initial release from halite and waste salt inclusions exposed at the surface. The dissolution behavior of the glass phase and the effective encapsulation of halite and other salt inclusion phases will determine the long-term performance of CWF and ACWF materials. Initial tests were conducted with CWF-P5-8 and CWF-C1-8 to demonstrate the behavior of "standard" CWF materials to which the responses of ACWF materials can be compared. The initial evaluation of ACWF materials was focused on the distribution and incorporation of salt constituents into inclusion phases and the glass, and the durability of the binder glass phase. Short-term tests were used to optimize the binder glass formulation and processing parameters.

The dissolution behaviors of the CWF and ACWF materials are being evaluated by using modified ASTM-International (ASTM) C1308, C1220, and C1285 test procedures (ASTM 2015a, 2015b, 2015c). The ASTM C1308 method was developed to evaluate diffusion-controlled releases as an improvement of the ANS/ANSI 16.1 method (ANS 2012), in which the test solution is replaced with fresh leachant at various prescribed durations. The replacement schedule called for in the ANSI restricts use of the results to empirical comparisons and prevents extraction of kinetic information. Kinetic information can be extracted from ASTM C1308 tests in which the test solution is replaced at constant test intervals to determine whether the release is controlled by diffusion (leaching) or uniform surface dissolution. The ASTM C1308 test method has been shown to be useful for evaluating the dissolution kinetics of waste glasses and CWF materials (Ebert and Snyder 2015).

The ASTM C1220 and C1285methods were developed to evaluate the dissolution behaviors of different materials in solution-dominated and solids-dominated static systems. These are used, respectively, to evaluate the effects of slow and rapid build-up of dissolved concentrations on the dissolution behavior. The ASTM C1308 tests provide mechanistic insights and distinguish the effects of solution feed-back

from the intrinsic dissolution behavior, whereas the ASTM C1220 and C1285 tests provide empirical demonstrations of the corrosion mechanism under extreme conditions.

4.2 Test Matrix

The test matrix is summarized in Table 11, where the values in the field indicate the S/V ratios (m^{-1}) used in the test and range of test intervals (days).

Table 11. Matrix of tests with CWF and ACWF materials

	Test Method:	C1308		C1220		C1285	
Material	Solution [a]	S/V, m^{-1}	Interval, d	S/V, m^{-1}	Duration, d	S/V, m^{-1}	Duration, d
CWF-P5-8	DIW, 1, 2, 3	7, 14, 20	1, 7	✓ [b]	✓ [b]	✓ [b]	✓ [b]
CWF-C1-8	DIW, 1, 2, 3	7	1, 7	—	—	✓ [b]	✓ [b]
CWF-P1-8	DIW	10	1	—	—	—	—
CWF-P6-8	DIW	10	1	—	—	—	—
ACWF-N2-11	DIW	10	1	—	—	—	—
ACWF-N3-11	DIW	10	1	—	—	—	—
ACWF-N4-11	DIW	10	1	—	—	—	—
ACWF-N5-11	DIW	10	1	—	—	—	—
ACWF-N6-11	DIW	10	1	—	—	—	—
ACWF-N4F-11	DIW	10	1	6, 12	1-120	2300	7
ACWF-N4-12	DIW, 1, 2, 3	10	1,7	6, 12	1-120	2300	7-56
ACWF-N4G-10	DIW, 1, 2, 3	10	1,7	6, 12	1-120	2300	7-56
ACWF-N4-14	DIW	10	1	6, 12	1-120	2300	7

[a] Solutions 1, 2, 3 = 10, 20, 30 ppm Si solution, respectively, and DIW = demineralized water.
[b] Tests conducted previously as part of CWF development.

Demineralized water (DIW) is used for all C1220 and C1285 tests and for most C1308 tests. Some of the C1308 tests with the CWF-P5-8 and CWF-C1-8 products made with P57 and Corning 7056 glasses were conducted in solutions prepared with high concentrations of dissolved Si, Na, and K to distinguish the dissolution behaviors of the sodalite and glass phases: sodalite dissolution is suppressed by even relatively low concentrations of dissolved Si that have only a small effect on the glass dissolution rate. Similar tests are planned with ACWF-N4-12 and ACWF-N4-13 products when the latter product is available. The Si solutions were made using a recently published method in which a potassium silicate glass is made and then dissolved to generate the desired solutions (Gin et al. 2015). Appropriate masses of that glass were dissolved to generate solutions with approximately 10, 20, and 30 mg Si L^{-1} (ppm). The pH values of these solutions were then adjusted to near 8.5 by adding small amounts of nitric acid or sodium hydroxide (pH 8.5 is near the "natural pH" attained when CWF materials dissolve in C1220 tests). The measured compositions of these solutions are summarized in Table 12. Analysis of the solutions

Table 12. Measured compositions of Si solutions

	10 ppm Si solution	20 ppm Si solution	30 ppm Si solution
Si	9.33	16.6	28.1
Na	3.41	6.6	9.17
K	99.9	184	263

(which was not done until the test solutions were analyzed) indicated high Na concentrations from both the addition of NaOH during pH adjustment and as contamination of the reagent KOH that was used to make the source potassium silicate glass. All concentrations are lower than the targeted values, but provide the desired range to distinguish the effects on the sodalite and glass dissolution rates. These are referred to as the 10, 20, and 30 ppm Si solutions for convenience, even though the actual concentrations are lower. The high Na and K concentrations are not expected to affect the glass dissolution rates and the solution pHs were adjusted to similar values. A new batch of the potassium silicate glass made using reagents with higher purity will be used in future tests.

In the initial tests conducted with CWF-P5-8 and CWF-C1-8 to establish the behavior to which the ACWF will be compared, the solutions were replaced daily for the first 11 days and then after three 7-day intervals to determine if degradation is controlled by surface dissolution or diffusion kinetics. Diffusion-controlled and surface dissolution-controlled releases are most readily distinguished by the results of the initial exchanges. The geometric surface area-to-solution volume (S/V) ratio of the specimen[6] will affect the test response for surface dissolution-controlled reactions because it affects the concentrations that are attained during each interval. The S/V ratio has a smaller impact on diffusion-controlled release since the concentration gradients are similar for all solutions. Tests conducted at different S/V ratios provide confirmatory evidence regarding the dissolution kinetics. The dissolution rates of sodalite and glass will be affected to different extents by the same dissolved silica concentration.

Short-term series of tests with daily solution exchanges were sufficient to compare the degradation behaviors of the prototype ACWF materials. Longer tests were conducted with the CWF materials to demonstrate the utility of the method, including tests using the Si solutions to confirm the attenuating effects of the solution composition, for later comparisons. More extensive testing is planned for ACWF materials made with higher waste loadings using the binder glass selected based on Phase 1 tests.

Specimens of all materials were cut and polished using absolute ethanol as the cutting fluid to avoid dissolving salt inclusion phases. The CWF and ACWF materials were cut from large pieces on six sides by using a low-speed wafering saw with a high density diamond blade. All sides of the CWF and the ACWF materials made with 11% salt loadings were polished sequentially with 240, 320, 400, and 600-grit abrasive paper using absolute ethanol as the lubricant. The ACWF materials made with higher salt loadings and with the size-reduced zeolite 4A were not polished prior to testing.

All tests were conducted in Teflon vessels at 90 °C in the same convection oven. Screw-top digestion vessels with internal volumes of about 100, 60, and 22 mL were used to achieve a range of S/V ratios. Teflon support grids were used in all vessels to provide free access for water to contact most of the surface. Solutions were exchanged within two minutes. Vessels were removed from the oven and weighed, then opened and most of the solution poured into two tared solution bottles for solution composition analysis and pH analysis. The last drop of solution was poured through a Teflon support mesh placed on a waste solution bottle to catch the specimen if it happened to fall out. The specimen was not dried during the exchange. The specimen was placed back into the vessel and fresh leachant was added. The mass of leachant was not measured independently. Rather, the vessel was filled to attain the same total mass as when the test was initiated to account for the small amount of solution carried over on the support grid and specimen at each exchange. This provides negligible contamination to the fresh leachant and minimizes what is considered to be the more significant effect of the sample drying. The vessel was recapped and tightly sealed. It is estimated that the test solution in the largest vessels reaches

[6] The geometric surface area was based on the dimensions of a specimen and does not include porosity. Since the porosities of the ACWF products are similar, the geometric S/V ratio provides a convenient and representative means to compare the test results.

90 °C less than an hour after the vessel is placed in the oven. Regardless, all tests experience the same temperature profiles. The Cl^- concentrations were measured by using an ion selective electrode; all other constituents were measured by using ICP-MS. The reacted test specimens have been retained for possible solids analyses.

4.3 Test Results and Discussion

Test results are evaluated in terms of the normalized elemental mass loss values calculated for each test interval (i.e., after each solution exchange). The normalized elemental mass loss function NL(i) utilizes the concentration of a soluble element *i* measured in the test solution to represent the mass of the material being tested that had dissolved. Comparing the NL(i) values calculated using different species indicates whether dissolution is stoichiometric. The dissolved mass is normalized to the geometric surface area of the test specimen to provide a value that can be used to compare tests with different specimen areas and scaled to the area of a full-size waste form. Dissolution occurring in each of a series of test intervals is referred to as the incremental normalized mass loss and is calculated as

$$\textit{incremental } NL(i)_n = \frac{C(i)_n}{S/V\, f(i)}, \tag{5}$$

where $C(i)_n$ is the concentration of species *i* measured in the test solution during test interval *n*, *S* is the geometric surface area of the test specimen, *V* is the volume of test solution, and $f(i)$ is the mass fraction of species *i* in the CWF or ACWF material used in the test. Values of NL(i) are presented as g m^{-2} and represent the masses of the CWF or ACWF materials that have dissolved during the test interval, not the masses of species *i* that have been released. These values allow for direct comparisons of materials having different compositions (i.e., different binder glass compositions or salt waste loadings) in tests conducted at different S/V ratios and with different exchange intervals.

For the ASTM C1308 tests, the cumulative dissolution occurring through a series of *n* test intervals is calculated as the sum of the incremental $NL(i)_n$ values as

$$\textit{cumulative } NL(i) = \sum_n NL(i)_n \,. \tag{6}$$

A maximum NL(i) value is established by the test specimen used in a test that is equal to the inverse of its specific surface area. The maximum NL(i) values for the ASTM C1308 and C1220 tests being conducted are summarized in Table 13. These values put the test results into perspective of the dissolved mass

Table 13. Maximum NL(i) values attainable in tests with CWF and ACWF products, in g/m^{-2}

C1308 Tests							
P6-11	N2-11	N3-11	N4-11	N5-11	N4F-11	N4-12	N4-14
1925	2031	1818	1477	2133	2586	2194	2098

C1220 Tests					
N4F-M6	N4F-M12	N4-12-M6	N4-12-M12	N4-14-M6	N4-14-M12
2211	1891	1617	1530	1990	1850

fractions that would be used as source terms for performance calculations. For the present purpose, they indicate the small fractions of the specimens that have reacted. The specific surface areas for crushedmaterials used in PCT will be measured before those tests are initiated to determine the upper limits for those tests. The available results for materials made with different binder glasses are discussed in the following sections. Tabulated test data and results for these and on-going tests will be provided in a subsequent report.

4.3.1 CWF Materials Made with P57 and Corning 7056 Glasses

Products CWF-P5-8 made previously with P57 glass and CWF-C1-8 made with Corning 7056 glass were subjected to ASTM C1308 tests conducted with ten 1-day exchange intervals followed by three 7-day exchange intervals. Figures 12a and 12c show the results for the first 10 intervals and Figures 12b and 12d show the results for the complete test durations in terms of incremental release. The first test intervals give significantly higher values of NL(Cl) and NL(Na) than all subsequent intervals through

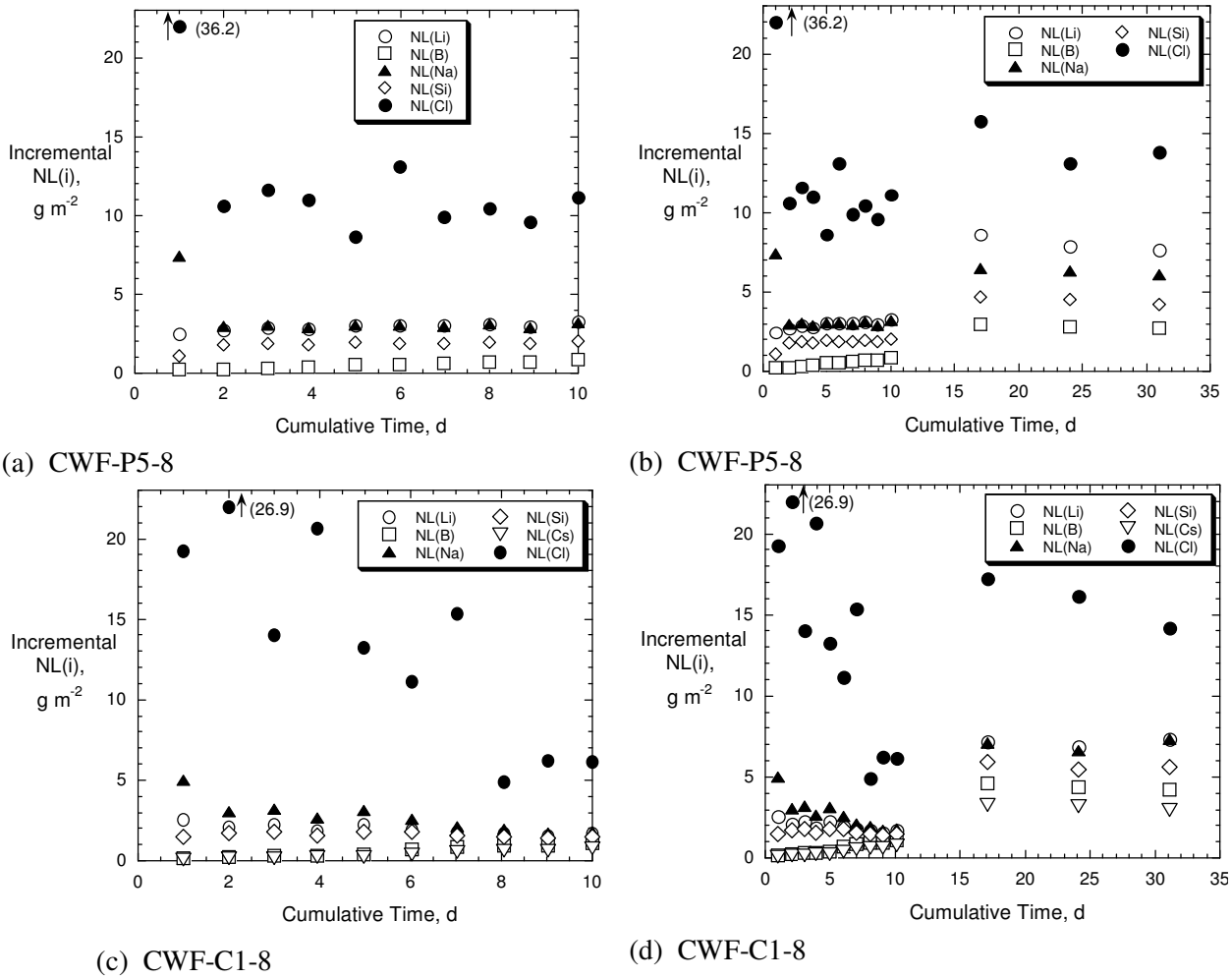

Figure 12. Incremental results for ASTM C1308 tests with CWF-P5-8: (a) initial ten 1-day exchange intervals and (b) ten 1-day intervals followed by three 7-day intervals and with CWF-C1-8: (c) initial ten 1-day exchange intervals and (d) ten 1-day intervals followed by three 7-day intervals.

10 d, which become nearly constant within the analytical uncertainty. The NL(i) values for other elements are essentially constant for all 1-day intervals, although values increase slightly for some elements and decrease slightly for others. The incremental NL(i) values of all elements increase significantly when the solution replacement interval is increased from 1 to 7 days, but remain nearly constant in subsequent 7-day exchanges. The slight decrease in the results for some elements during the second and third 7-day intervals is attributed to analytical uncertainty and the decrease in reactive surface area. It does not indicate diffusion-limited release because no diffusive character was seen during the 1-day exchanges.

Figure 13 shows the results of ASTM C1308 tests conducted with materials CWF-P5-8 m and CWF-C1-8 expressed as cumulative release. Note that these and all subsequent plots are for cumulative NL(i) values, although this is not shown on the *y*-axis labels of the plots. We emphasize that the slopes of these plots reflect the release kinetics but **do not give the release rates of the elements**. Rather, linear increases in the cumulative NL(i) values indicate linear release kinetics and sub-linear (e.g., root-time) behavior in the cumulative NL(i) values would indicate diffusive release kinetics. The release behaviors of B, Li, Na, Si

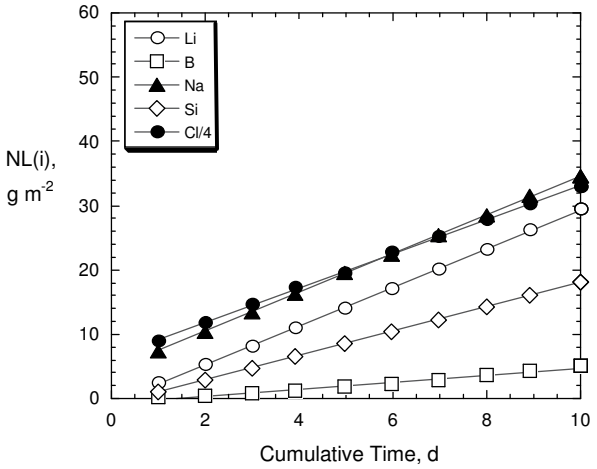

(a) CWF-P5-8

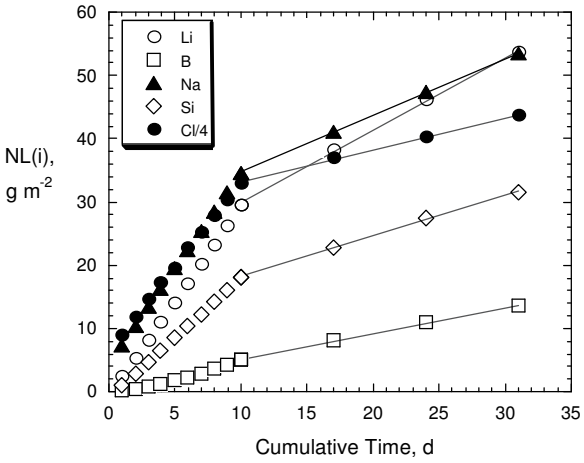

(b) CWF-P5-8

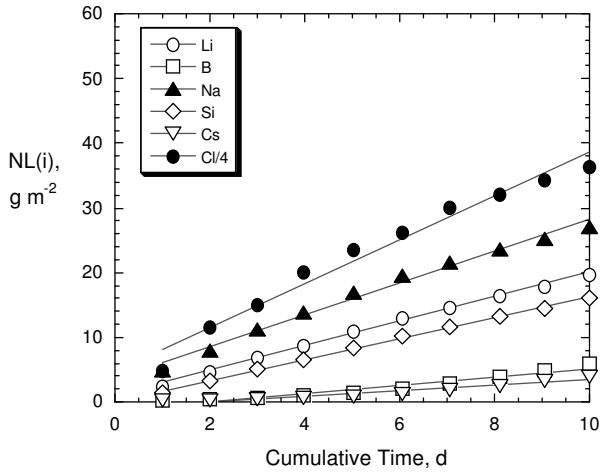

(c) CWF-C1-8

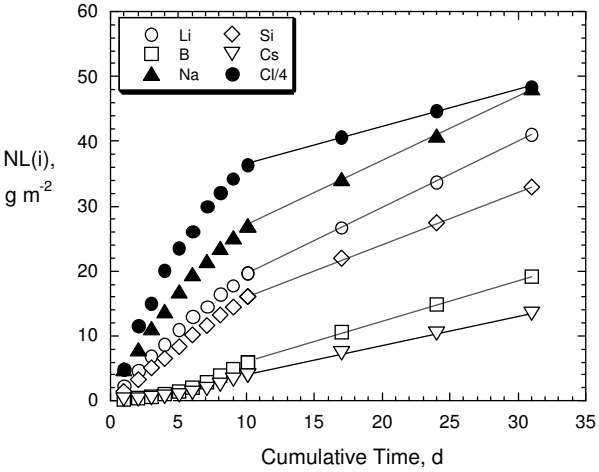

(d) CWF-C1-8

Figure 13. Cumulative results for ASTM C1308 tests in DIW: (a) and (b) with CWF-P5-8 at 14 m^{-1} and (c) and (d) with CWF-C1-8 at 7 m^{-1}.

and Cl^- are similar and slightly slower in tests with CWF-P5-8 than with CWF-C1-8 due, in part, to the higher S/V ratio. The releases of all elements are nearly linear during the first 11 days when the solutions are exchanged daily and then through 31 days when the solutions are exchanged weekly. The initial releases of Li, Na, and Cl^- from CWF-C1-8 may indicate slight diffusive character, but the behavior at longer test durations does not support this mechanism. The release is probably linear within the testing uncertainty. The smaller slopes for the 7-day exchanges indicate lower dissolution rates due to solution feedback. Notice that the NL(Na) and NL(Cl) are higher than the other NL(i) after the first interval in tests with both materials. This is attributed to the immediate dissolution of a small amount of halite at the surface. Less halite is present in the CWF-C1-8 product.

The effect of the dissolved silica concentration on the dissolution behavior was studied by conducting ASTM C1308 tests in various KH_2SiO_4 solutions. The results of ASTM C1308 tests with CWF-C1-8 in the various Si solutions are shown in Figure 14. The same test series was completed with CWF-P5-8 but not yet been analyzed. Data are plotted on the same scale to facilitate direct comparisons. The Si and Na

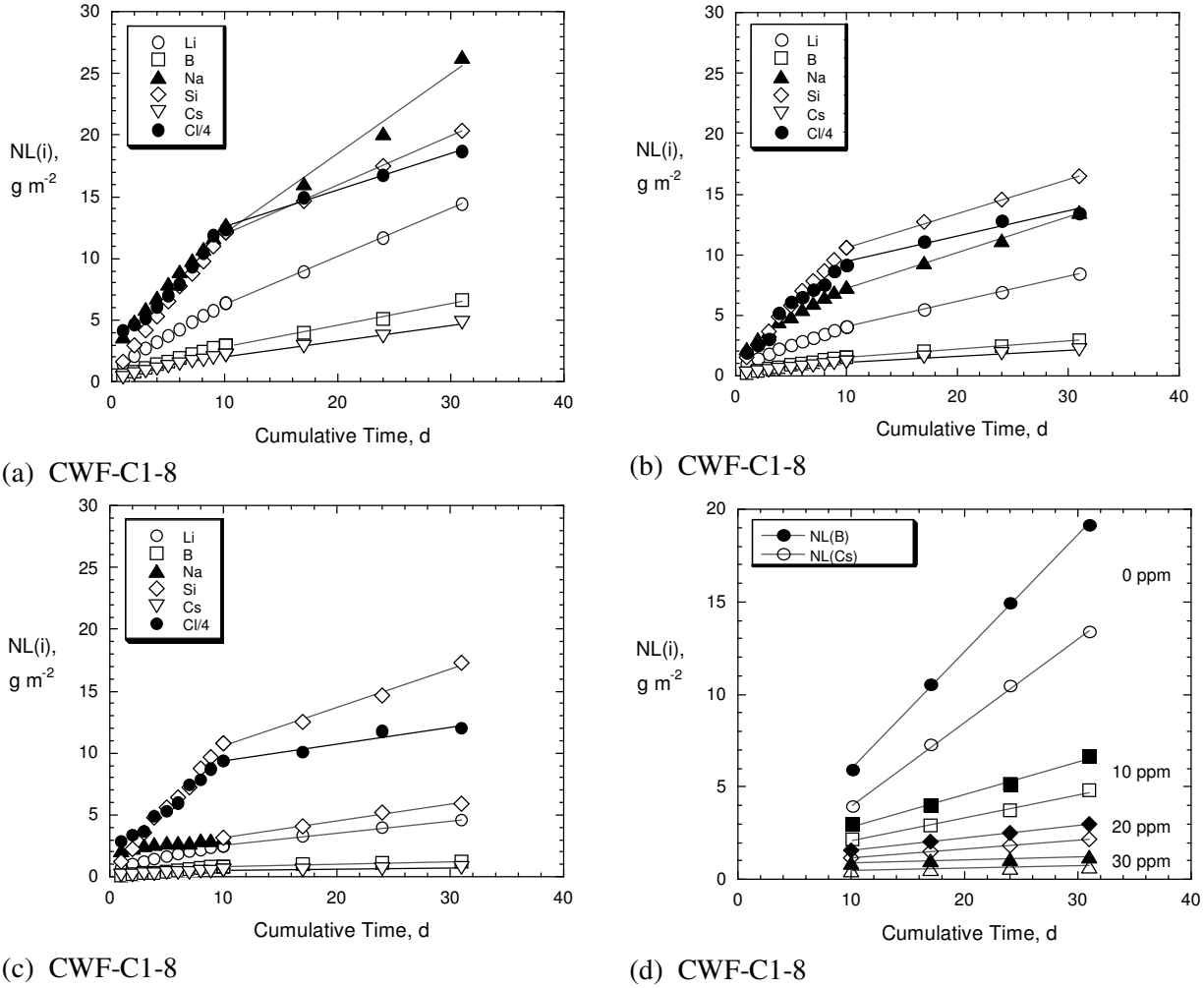

(a) CWF-C1-8

(b) CWF-C1-8

(c) CWF-C1-8

(d) CWF-C1-8

Figure 14. Cumulative results for ASTM C1308 tests with CWF-C1-8 at 7 m^{-1} in (a) 10 ppm Si solution, (b) 20 ppm Si solution, (c) 30 ppm Si solution, and (d) NL(B) (solid symbols) and NL(Cs) (open symbols) in the four solutions.

concentrations have been background-adjusted to account for the spiked concentrations and have higher uncertainties than the NL(i) values for the other species. The releases of all species decrease significantly in the 10 ppm Si solution compared with tests conducted in DIW (see Figure 13d) and decrease further in tests with the higher Si concentrations. The observation that the decrease is not linear with the Si concentration is interpreted to indicate the 10 ppm Si solution almost completely attenuates the sodalite dissolution and the 20 and 30 ppm Si solutions only affect the glass dissolution. Figure 14d provides direct comparisons of NL(B) and NL(Cs) for tests conducted in DIW and the three silicate solutions. Relative to the cumulative extent of B dissolved in DIW through the 31-day test period, the 10, 20, and 30 ppm solutions attenuate dissolution by 65, 79, and 89%. The effect on the release of Cs is proportional to that of B, which indicates most of the Cs is in the glass phase.

4.3.2 Phase 1 ACWF Products Made with P57 and NBS Glasses

The results of abbreviated ASTM C1308 tests conducted with the initial prototype ACWF materials made with the new binder glasses are shown in Figures 15 to compare the release behaviors of different elements from each product. The general release behavior of each element is similar for materials made

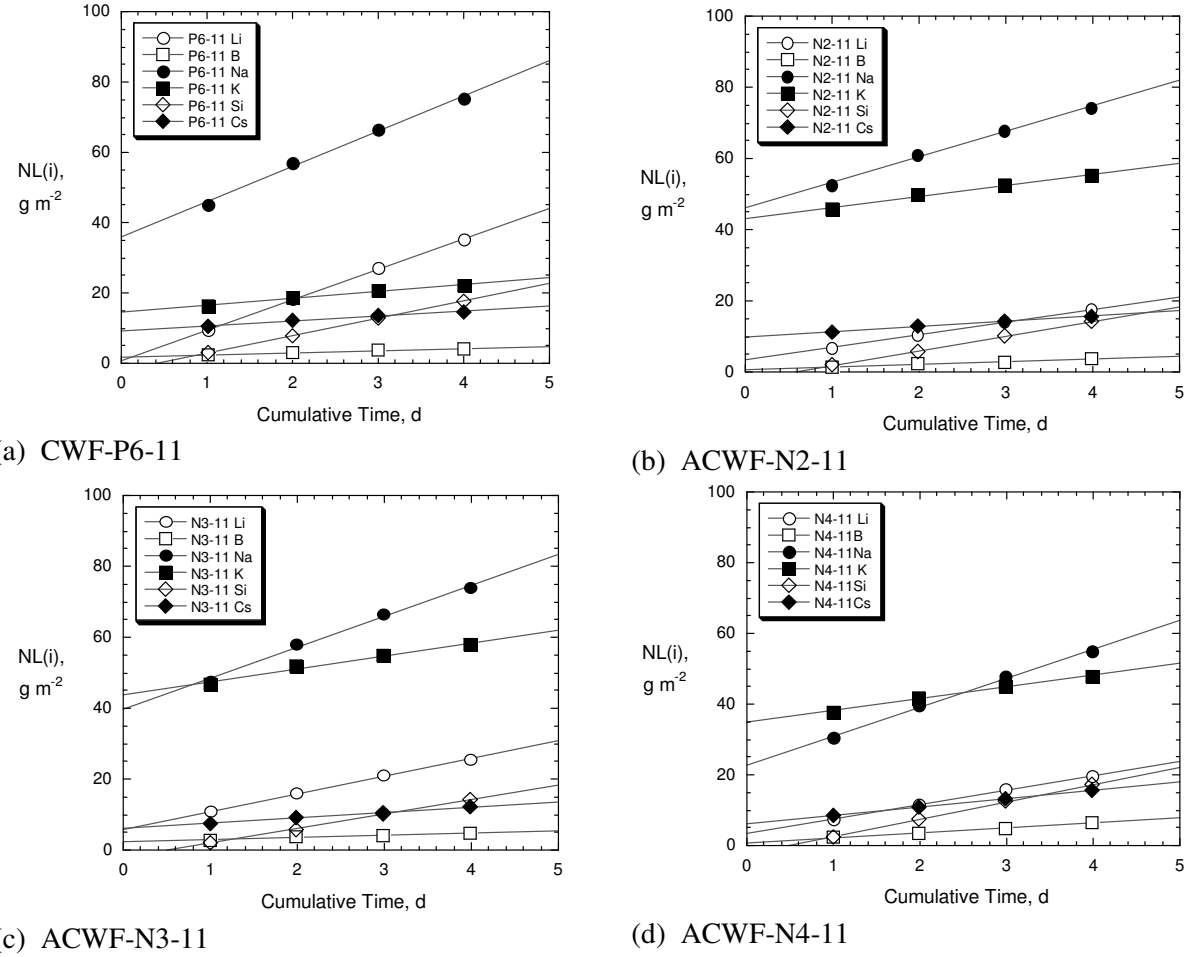

(a) CWF-P6-11

(b) ACWF-N2-11

(c) ACWF-N3-11

(d) ACWF-N4-11

Figure 15. Cumulative results for ASTM C1308 tests in DIW at 10 m^{-1} with (a) CWF-P6-11, (b) ACWF-N2-11, (c) ACWF-N3-11, (d) ACWF-N4-11, and (e) ACWF-N5-11.

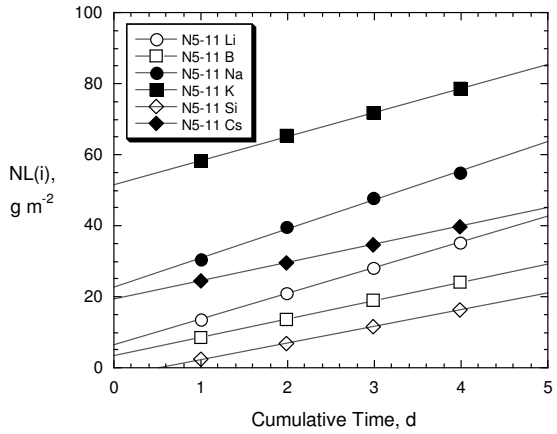

(e) ACWF-N5-11

Figure 15. (cont.)

with each NBS glass: all species are released with linear kinetics; the values of NL(Cl) are higher than the NL(i) values for other species; the release rates of the different elements (which are related to the slopes of the lines) are similar, but the *y*-intercepts differ; the slopes of NL(Cl) and NL(Li) are highest and the slopes of NL(B) and NL(Cs) are lowest; and the *y*-intercept is negative for NL(Si) but positive for other NL(i) of the other elements.

The interpretation of degradation behavior revealed in these test results is as follows. Consider first the values of NL(Cl) for the five materials with 11% waste salt loadings, which are compared in Figure 16a. The slopes are seen to be very similar but the *y*-intercepts differ. The *y*-intercepts are interpreted to represent the rapid dissolution of halite (NaCl) and unincorporated salt exposed at the outer surfaces of the test specimens. Complete dissolution of the exposed salt inclusion phases occurs within the first few minutes after the ACWF is contacted by water and occurs as a one-time pulse during the first test interval. The *y*-intercepts represent the concentrations generated assuming dissolution of these phases is instantaneous and are proportional to the amounts of soluble inclusion phases that are exposed at the specimen surface and in connected pores. The fractional surface areas of the inclusion phases are assumed to be equal to the volume fractions of those phases in the bulk ACWF materials. That assumption is supported by the area and volume porosity reported in Table 9. Comparing the *y*-intercepts indicates that ACWF products made with NBS-2, NBS-3, and NBS-5 contain the most accessible halite and/or unincorporated salt and that the ACWF products made with NBS-4 and P57 (P6) glass contain smaller amounts of highly soluble inclusion phases.

Whereas the dissolution of halite at the specimen surface dominates the initial interval, subsequent intervals are dominated by dissolution of sodalite and glass. The linearity of data in Figure 16a indicates the release rate of Cl^- becomes constant after the first exchange. Essentially all of the Cl^- released into solution after the first interval is due to dissolution of sodalite. The red arrows illustrate how the NL(Cl) data are interpreted to represent the sum of contributions from different phases in the test with ACWF-N4-11. It starts with the immediate dissolution of exposed halite and unincorporated salt, which provides a transient pulse represented by the *y*-intercept, and continues the slow dissolution of sodalite, which represents the small increase during each interval. The plots show that the high release occurring during the first interval does not occur again in subsequent intervals. We emphasize that the slopes do not provide the dissolution rates because the solutions are exchanged daily. Rather, the linear slopes for all elements indicate the same extent of release occurs during each interval and that the reactivity of the

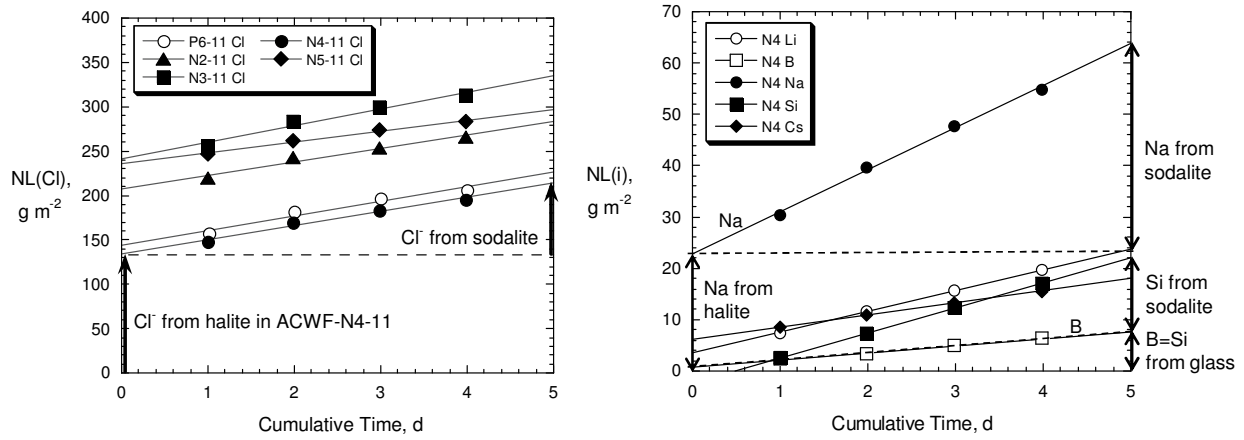

(a) (b)

Figure 16. Analyses of cumulative results of ASTM C1308 tests to estimate contributions of (a) Cl^- release from halite and sodalite and (b) Na release from halite and sodalite, B release from glass, and Si release from sodalite and glass phases in ACWF-N4-11.

surface remains constant. This indicates the Cl^- release is controlled by a surface dissolution process with no significant effect of mass transport or diffusion limitation. The contribution of glass phase dissolution to the Cl^- release is small because only a small amount of Cl^- can dissolve into the glass (about 1 mass%). However, halite that is encapsulated in the glass will be released when the surrounding glass dissolves to expose it to water. From a modeling perspective, material in halite inclusions can be considered to be dissolved in the glass. The contribution of glass dissolution is determined from the B release, which is discussed next.

Consider next the dissolution behavior of the sodalite and glass phases, which is discussed using the results for ACWF-N4-11 given in Figure 16b. Values of NL(B) are used to represent dissolution of the glass phase because B is only present in the glass. These results show B is released at a constant rate, which is used to represent the overall glass dissolution kinetics. Si is present in the sodalite and glass, but the amount released from the glass can be assumed to be stoichiometric with B under these highly dilute test conditions, so the difference between NL(Si) and NL(B) can be used to represent the release of Si from sodalite. Following the same logic used to describe th Cl^- release, the amount of Na released by halite dissolution is given by the *y*-intercept of the NL(Na) plot and the amount released due to dissolution of sodalite and glass is given by the increases in subsequent test intervals. The observation that the slopes of NL(Na) and NL(Si) are similar is consistent with the interpretation that most of the Na and Si are released by sodalite and glass dissolution. Since almost all of the Na was removed from the glass to make sodalite in these ACWF materials, the released Na is assumed to be due almost exclusively to the dissolution of halite and sodalite. Furthermore, comparing the NL(Na) and NL(Cl) values indicates the contribution of glass dissolution (including halite inclusions) to the Cl^- release is negligible.

Figure 17 shows plots comparing the releases of key elements from the different CWF and ACWF materials, which can be interpreted using the phase analysis just described. Plots for NL(Na) and NL(K) have appreciable *y*-intercept values that indicates these elements are presence in salt inclusion phases, whereas plots for NL(Li), NL(B), and NL(Si) have *y*-intercept values near zero that indicate they are not. The slopes of NL(Si) for all ACWF materials are higher than that for CWF-C1-8. This is attributed to the greater amounts of sodalite in all ACWF materials leading to more sodalite surface area being exposed in tests conducted with those materials.

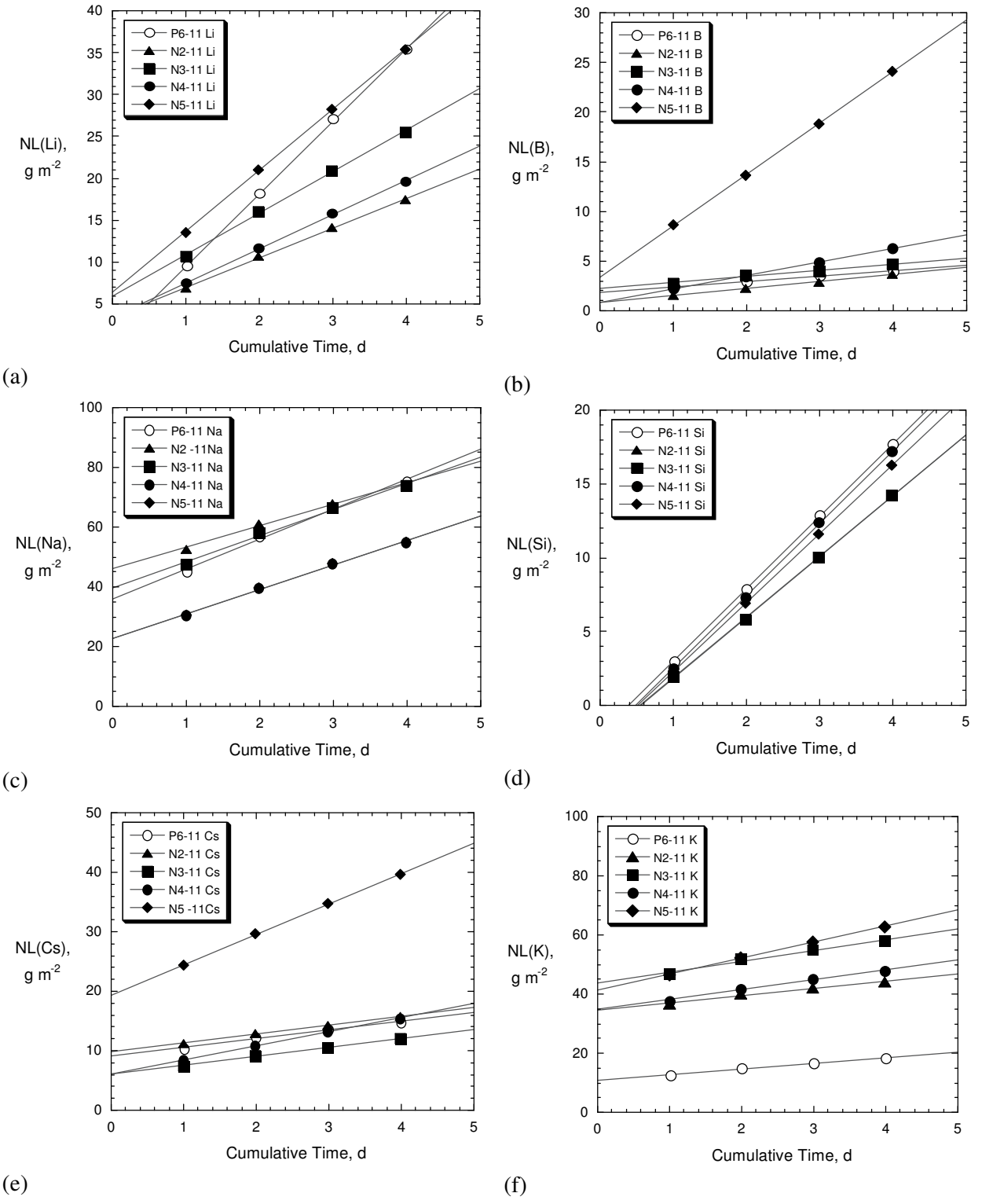

Figure 17. Cumulative results for ASTM C1308 tests with different ACWF materials with 11% waste salt loading: (a) NL(Li), (b) NL(B), (c) NL(Na), (d) NL(Si), (e) NL(Cs), and (f) NL(K).

The results in Figures 16 and 17 also provide a qualitative comparison of the relative durabilities of these five materials. The most halite is generated in ACWF-N3-11 based on the *y*-intercepts of NL(Cl) and NL(Na) plots. The glass phase is significantly less durable in ACWF-N5-11 than in the other materials based on the slopes of NL(B), NL(Li), and NL(Cs). The durabilities of the sodalite phases in all materials are similar based on the similar slopes of NL(Na), NL(Si), and NL(Cl).

The ASTM C1308 tests provide insights into the disposition of Cs in the ACWF materials that was not available from direct solids analyses. NL(Cs) has a positive *y*-intercept that may indicate a small fraction of the Cs inventory is present in inclusions. However, NL(B) also has a positive *y*-intercept, which is likely an artifact of sample preparation, such as a small amount of fines due to polishing that remain on the specimen and dissolve when the test is started. The slopes of NL(B) and NL(Cs) are similar for dissolution of the various materials and lower than the slopes of NL(Na) and NL(Si). This indicates that sodalite is dissolving faster than the glass phase under these test conditions and that Cs is being released from in the glass phase. The slopes for different materials are very similar except for ACWF-N5-11, which has higher NL(B) and NL(Cs) slopes than the other materials. Based on the result of Lambregts and Frank discussed in Section 2, any Cs that is not incorporated into the glass is probably present as inclusions of unreacted salt rather than in halite; the similar *y*-intercepts of the salt constituents in these tests is consistent with this expectation.

The incorporation of Cs into a chemically durable phase is viewed as a major objective of the ACWF development because it represents key dose contributors and is one of the most soluble radionuclides in the salt waste. The first criterion used to select the NBS glass for Phase 2 materials was the incorporation of Cs. This included first the amounts of Cs released immediately (the *y*-intercepts) and then the continued releases as glass phases dissolved (the slopes). The Cs release behavior from the ACWF product made with NBS-5 glass was distinctively poorer than from products made with NBS-2, NBS-3, and NBS-4 glasses, which were similar, both in the *y*-intercept and the slope. NBS-5 was eliminated from consideration. The next criterion was the estimated amount of halite generated, which is inversely proportional to the amount of sodalite. The *y*-intercepts of NL(Cl) were lowest for products made with NBS-4 and P57 glasses, and the *y*-intercept of the NL(Na) plot is lowest for the product made with NBS-4.

It is important to note that the performance of most ACWF materials in these tests is similar to that of CWF-P6-11 even though about twice the amount of sodalite is generated to incorporate Cl^- and half as much glass remains in the ACWF materials (see Table 9). NBS-4 was selected for use in the Phase 2 materials.

4.3.3 Phase 2 ACWF Products Made with NBS-4 Glass

The Phase 2 materials were formulated to evaluate the maximum salt waste loading and decrease the porosities of the ACWF products. Since it was expected that an acceptable material could be made with about 12 mass% loading of the ER salt, materials were made with 12% and 14% salt loadings. A salt waste loading that is higher than the theoretical maximum loading based on reaction stoichiometries discussed in Section 1 was used to determine the effects of using a too-high salt loading on the physical properties and chemical durability. The high porosity in the Phase 1 ACWF materials was attributed to the relative volume of the sodalite and glass phases and the size of the sodalite domains. The size of the sodalite domains in the CWF and ACWF materials appeared to be determined by the size of the aggregated particles of zeolite 4A. Since the glass fills the voids between these domains, it was reasoned that the porosity of the ACWF materials could be decreased by using smaller aggregates of zeolite 4A. To evaluate this expectation, the ACWF-N4F-11 product was made with zeolite 4A that had been crushed to -200 mesh size (<45 µm) prior to salt occlusion and the NBS-4 glass had been crushed to the same size. A salt loading of 11 mass% was used to allow direct comparison with ACWF-N4-11 to evaluate the benefit of a smaller zeolite 4A size.

Figures 18 and 19 show the results of ASTM C1308 tests conducted with ACWF materials made for Phase 2 testing with NBS-4 glass and different salt loadings and with finely crushed zeolite 4A. The same test results are plotted in Figure 18 to compare releases of different elementals from each material and plotted in Figure 19 to compare the releases of each constituent from the different materials. Results for the Phase 1 material ACWF-N4-11 are included for comparison and all plots are presented on the same scale to facilitate visual comparisons. The relative release behaviors of the different elements are generally the same for the Phase 2 materials as was observed for the Phase 1 ACWF materials, except for one important exception: the NL(Cs) values for ACWF-N4-14 are similar to the NL(Na) and NL(K) values. The distinct release behaviors of these elements from ACWF-N4-14 are most clearly seen in Figures 19c, 19e, and 19f. The slopes of the NL(B) and NL(Li) plot are interpreted to represent the relative durabilities of the glass phases in the different materials, and these results indicate that ACWF-N4F-11 is the least durable. It also has the highest NL(Cl) *y*-intercept, which indicates it has the highest halite content. The similar slopes of the NL(Na) and NL(Si) results indicate the durabilites of the sodalite phases in all materials are similar. The *y*-intercepts of NL(Cs), NL(K), and NL(Na) for different materials are correlated but the *y*-intercepts of NL(Cs), NL(Na), and NL(Cl) are not.

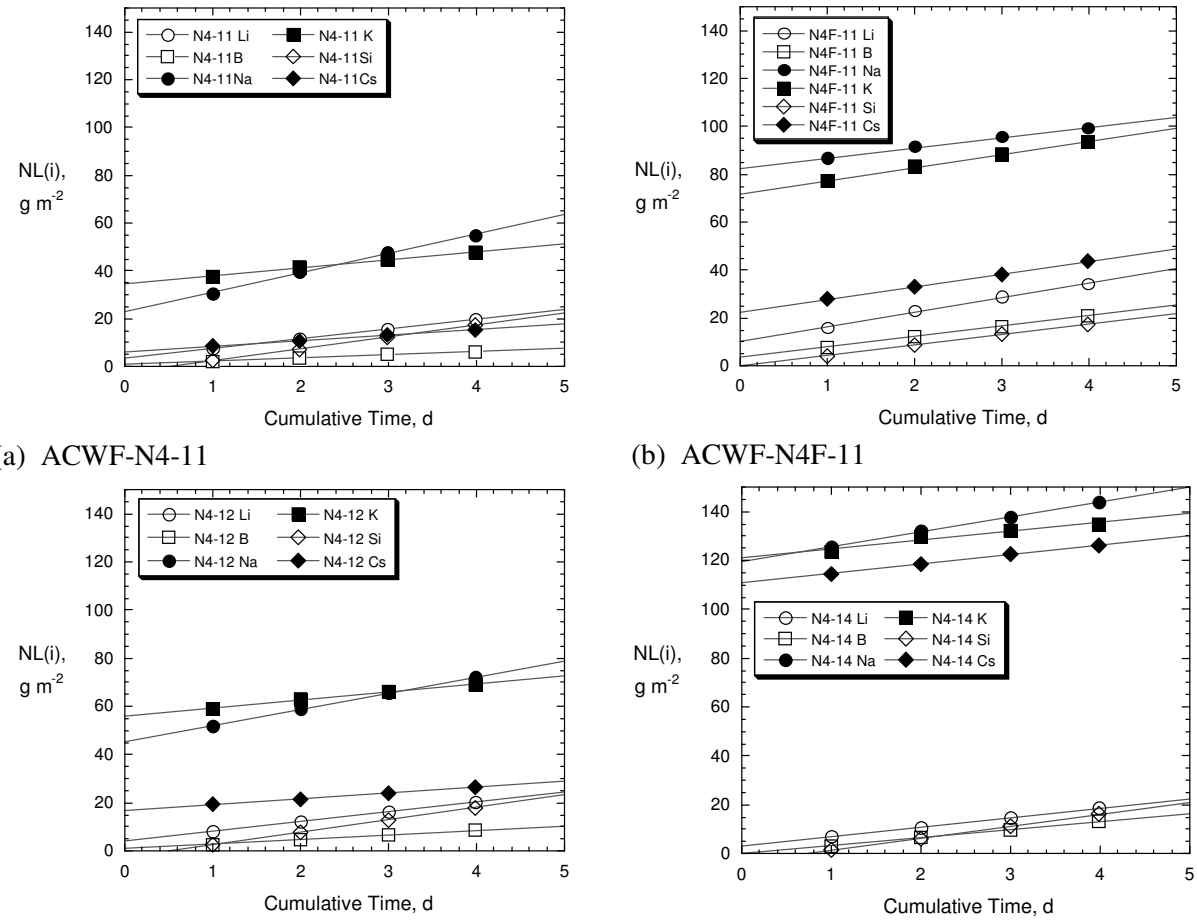

(a) ACWF-N4-11

(b) ACWF-N4F-11

(c) ACWF-N4-12

(d) ACWF-N4-14

Figure 18. Cumulative results for ASTM C1308 tests with (a) ACWF-N4-11, (b) ACWF-N4F-11, (c) ACWF-N4-12, and (d) ACWF-N4-14.

Overall, this indicates a significant fraction of Cs was not incorporated into the glass or halite phases in ACWF-N4-14, but instead was present in inclusions of residual unreacted waste salt. More importantly, this provides indirect evidence that Cs was incorporated into the glass phases in the other materials. As predicted, the 14% waste loading of ER salt exceeds the capacity of the ACWF but 12% waste loading does not. The impact of a too-high salt waste loading is simply incomplete incorporation of Cl^- into sodalite leading to the generation of waste salt inclusions in the glass phase. The ASTM C1308 test method is sensitive enough to detect the presence of these waste salt inclusions, although their presence was not revealed by XRD or microscopy. Establishing the effects of using a too-high salt waste loading allows for reliable determinations of maximum waste loadings of the ER waste salt and other waste salt compositions based on reaction stoichiometries, glass composition, and production controls that can be verified experimentally.

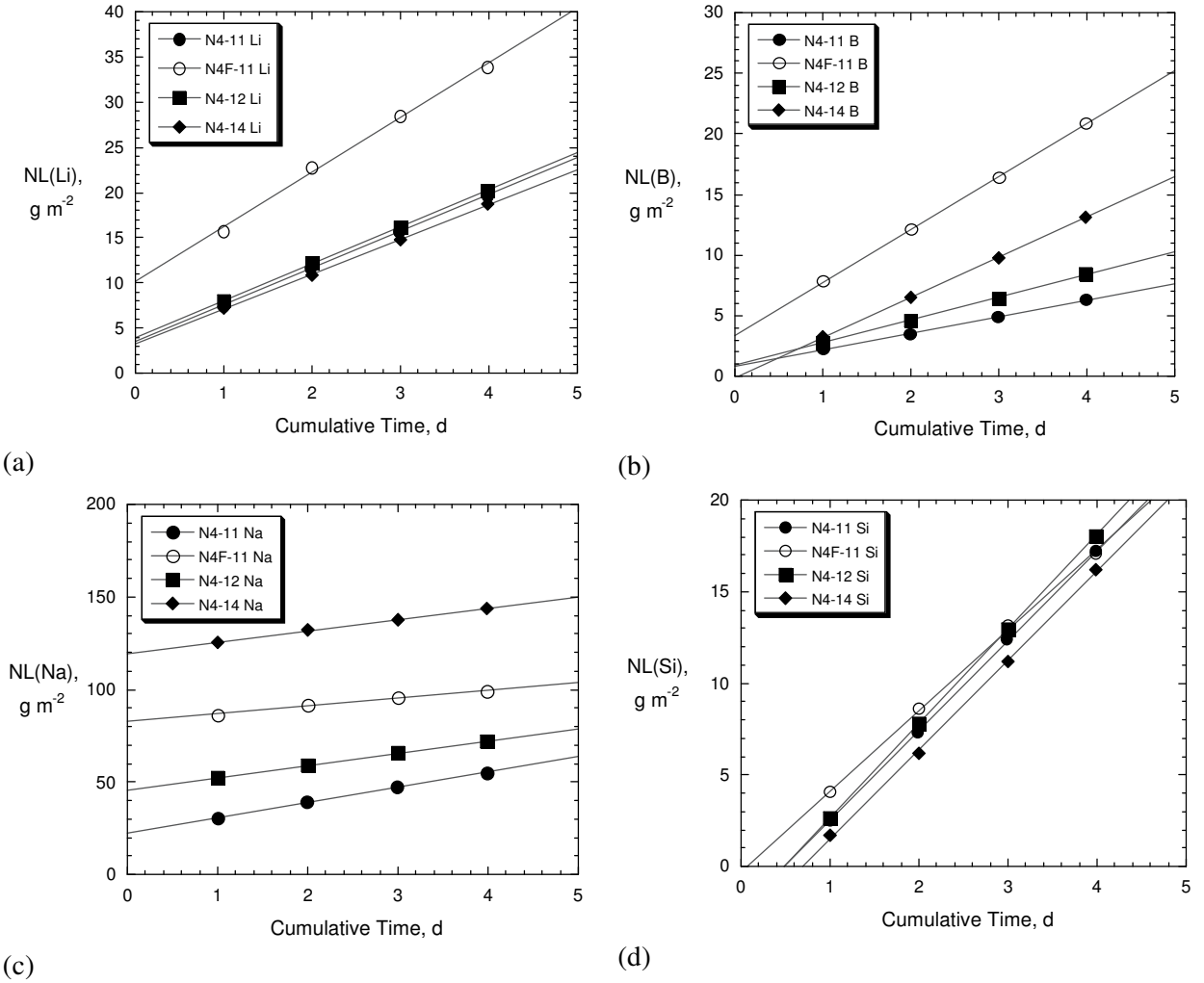

Figure 19. Comparisons of releases from different ACWF materials: (a) NL(Li), (b) NL(B), (c) NL(Na), (d) NL(Si), (e) NL(Cs), (f) NL(K), and (g) NL(Cl).

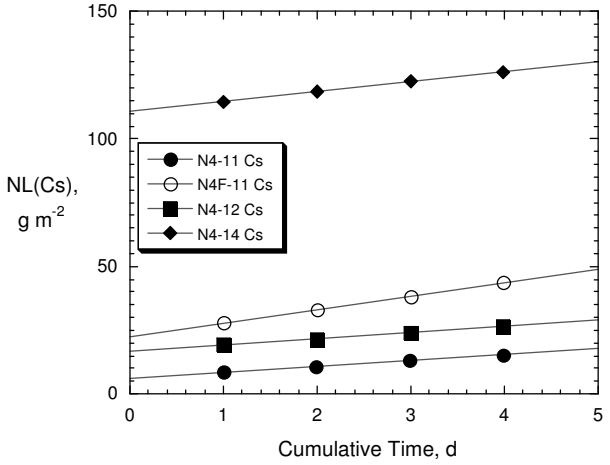

(e)

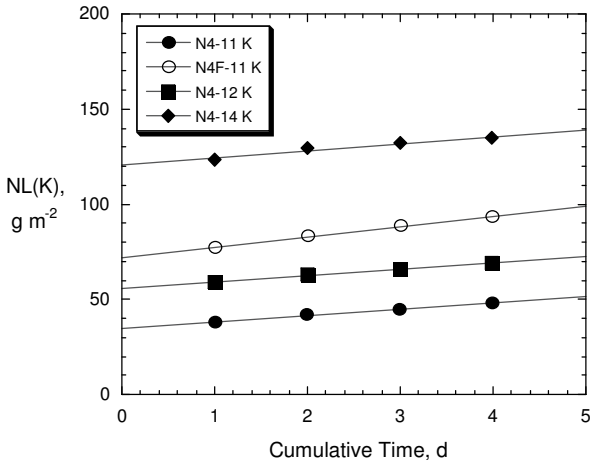

(f)

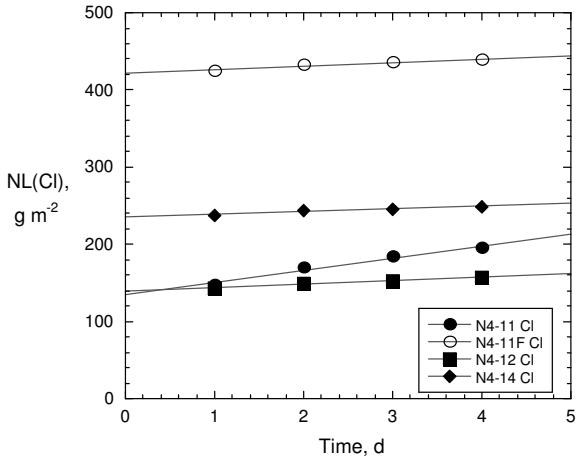

(g)

Figure 19. (cont.)

4.3.4 Planned Testing in Phases 3 and 4

The results of the Phases 1 and 2 tests indicate that the porosity will limit salt waste loadings to values within the capacity of the five NBS glasses that have been formulated, and that there is no need for a binder glass with a higher Na_2O content. Instead, additional ACWF materials will be made with higher fractions of binder glass to decrease the porosity of the product; as exemplified by ACWF-N4G-10. Although increasing the relative amount of binder glass will decrease the waste loading, the salt waste loading is not expected to change significantly (relative to the ACWF materials made to-date) on a per disposal canister basis because the volume occupied by the additional glass replaces void volume. A filled canister will have the same amount of waste salt despite the lower mass fraction.

The objective of Phase 4 testing is to demonstrate the flexibility of the ACWF to accommodate the extreme salt waste compositions that may occur during waste decontamination operations for salt recycle. In essence, these tests will determine if Li, K, Rb, Cs, Sr, and Ba will dissolve in glass or form separate $MAlSiO_4$ or celsian-like phases as discussed in Section 2.3. Simple salt compositions will be formulated

for use in demonstration tests to represent several relevant salt waste compositions that are predicted to be generated by various processing operations by simulation models being developed at INL. Insights gained from formulating ACWF materials for Phase 1 and Phase 2 testing will be applied to these waste salt compositions to predict the phase assemblages and the amounts of zeolite 4A and binder glass needed to support the chemical and physical requirements based on reaction stoichiometries and amounts expected to be generated.

The strategy for formulating and testing ACWF materials for extreme waste salt compositions is shown using a waste salt composition 97% LiCl + 2% $SrCl_2$ + 1% Li_2O on a mass basis. As described in Section 2.3, the disposition of LiCl is expected to depend on the efficiencies of competing reactions with zeolite 4A in the presence of a sodium borosilicate glass:

$$Na_{12}(AlSiO_4)_{12} + 3\ SiO_2 + 3\ LiCl \rightarrow 1.5\ Na_8(AlSiO_4)_6Cl_2 + 3\ LiAlSi_2O_6 \qquad \text{Reaction 16}$$

$$\text{glass}{\equiv}\text{SiO-Na} + LiCl \leftrightarrows \text{glass}{\equiv}\text{SiO-Li} + NaCl \qquad \text{Reaction 23}$$

$$Na_{12}(AlSiO_4)_{12} + 4\ NaCl \rightarrow 2\ Na_8(AlSiO_4)_6Cl_2 \qquad \text{Reaction 15}$$

$$Na_8(AlSiO_4)_6Cl_2 \rightarrow 2\ NaCl + 1.5\ Na_4(AlSiO_4)_4\,. \qquad \text{Reaction 3}$$

Reactions 23 and 15 must occur in preference to Reaction 16 to produce a reasonable waste form. Reactions analogous to Reactions 16 and 23 probably occurred with CsCl (Lambregts and Frank 2002, 2003):

$$Na_{12}(AlSiO_4)_{12} + 3\ SiO_2 + 3\ CsCl \rightarrow 1.5\ Na_8(AlSiO_4)_6Cl_2 + 3\ CsAlSi_2O_6 \qquad \text{Reaction 7}$$

$$\text{glass}{\equiv}\text{SiO-Na} + CsCl \leftrightarrows \text{glass}{\equiv}\text{SiO-Cs} + NaCl \qquad \text{Reaction 9}$$

such that separate Cs-free sodalite, Cs-pollucite, and Cs-rich glass phases were generated. It is important to note that Reactions 16 and 7 consume molar amounts of SiO_2 from the glass that are equivalent to the molar LiCl and CsCl contents in the salt. As seen the CWF materials made with CsCl by Lambregts and Frank, the loss of glass prevents it from encapsulating the crystalline phases that form. If Reaction 7 dominates, each gram of CsCl will consume 0.36 g SiO_2 and enrich the glass in B, Al, and alkalis. Lambregts and Frank showed significant amounts of Cs-pollucite (and sodalite) formed in CWF made with CsCl and with a 50/50 mixture of CsCl and NaCl, but not with a 25/75 mixture. Most of the Cs was in the glass phase of the CWF made with the 25/75 mixture. This suggests that CsCl dissolved into the glass phase preferentially and Cs-pollucite formed with CsCl the glass could not accommodate.

If Reaction 16 dominates, each gram of LiCl will consume 1.42 g SiO_2, which is about 4-times that consumed by CsCl. Lambregts and Frank reported that "appropriate amounts" of salt, zeolite, and glass were used, but did not specify if those were based on mass or molar proportions. Since they used CsCl/NaCl mixtures based on mass, it is assumed the salt, zeolite, and glass mixtures were mass-based.

The Sr^{2+} from $SrCl_2$ is predicted to exchange with Na^+ from the glass and then react with zeolite 4A to form stronsiocelsian as:

$$\text{glass}{\equiv}\text{SiO-Na} + 0.5\ SrCl_2 \leftrightarrows 0.5\ \text{glass}{\equiv}\text{SiO-Sr-OSi}{\equiv}\text{glass} + NaCl. \qquad \text{Reaction 12}$$

$$Na_{12}(AlSiO_4)_{12} + 1.5\ SrCl_2 \rightarrow 1.5\ Na_8(AlSiO_4)_6Cl_2 + 1.5\ SrAl_2Si_2O_8\,. \qquad \text{Reaction 14}$$

The formation of stronsiocelsian in Reaction 14 does not consume SiO_2 from the glass. The impact of LiCl and $SrCl_2$ in the salt is that sequestration of Cl^- is less efficient: 3 moles Cl^- are immobilized for every mole of zeolite reacted rather than 4 moles Cl^- by reaction with NaCl. More zeolite 4A is required

for salts with high LiCl contents and more glass is required to provide SiO_2 to form celsian-like phases and encapsulate the greater volume of crystalline phases.

The ACWF formulation will be based on the stoichiometries to provide enough zeolite 4A to generate enough sodalite in case Li- and Sr-aluminosilicates do not form, will provide enough glass to supply the SiO_2 required to generate enough Li- and Sr-aluminosilicates to accommodate all the Li and Sr in the salt if they do form, and provide enough NBS-4 glass to supply enough Na^+ to exchange with Li^+ and Sr^{2+} and accommodate those cations in the glass. The Li_2O in the salt is assumed to dissolve into the glass phase without affecting the reactions leading to formation of the silicates.

Table 14 provides representative recipes for Li-ACWF materials made with two salt compositions with high LiCl contents at low and high SLZ/glass ratios. These masses will produce 50-g products. The waste loadings for the salt with more Sr^{2+} are higher on a mass basis since Li^+ and Sr^{2+} replace Na^+ in the glass on a mole basis. These materials will show the propensity for Li^+ and Sr^{2+} to dissolve into the glass phase rather than form separate Li-aluminosilicates.

Table 14. Recipes for Li-ACWF

	97% LiCl + 2% $SrCl_2$ + 1% Li_2O		70% LiCl + 20% $SrCl_2$ + 10% Li_2O	
	Li-ACWF-1-1	Li-ACWF-1-2	Li-ACWF-2-1	Li-ACWF-2-2
SLZ/glass	1.25	2.0	1.25	2.0
Waste salt, g	2.5584	3.0700	3.0486	3.2925
Zeolite 4A, g	25.2194	30.2633	24.7292	26.7075
Glass NBS-4, g	22.2222	16.6667	22.2222	20.0000
Salt waste loading, mass%	5.12%	6.14%	6.10%	6.58%

These Li-ACWF materials were formulated to evaluate the chemistry and give insight to amount of glass needed to encapsulate the phases that are formed. They are intended to be diagnostic. Although materials were formulated to have more than enough glass to provide the Na^+ needed to exchange with Li^+ and Sr^{2+} and dissolve them into the glass and enough SiO_2 to generate the Li- and Sr-aluminosilicates, there may not be enough to encapsulate all the product phases if large amounts of aluminosilicates form. The ACWF products made to-date indicate that more than 26 mass% glass is required to encapsulate the amounts of sodalite formed at high loadings of ER salt waste. It is likely that previous attempts to make CWF materials using salts with high LiCl contents failed because they followed the recipe developed for ER salts. The salt loading is too high and the glass content is too low for salts with high LiCl contents; the Na_2O content of the P57 binder glass is also too low to provide the required Na^+. We expect ACWF materials made with the appropriate amounts of salt, zeolite 4A, and NBS-4 will accommodate salts with high LiCl contents and salts with concentrations of other constituents that are much higher than those in the ER waste salt.

5. CONCLUSIONS

The concept of using a binder glass with a high Na_2O content to provide Na^+ for generating sodalite to sequester Cl^- from the waste salt has been successfully demonstrated. However, the waste loadings for ACWF products made by processing at ambient pressures become limited by the amount of glass required to encapsulate the sodalite and attain acceptably low porosities. Modifications of the processing conditions and probably the glass/SLZ ratio used to make the ACWF products are required to improve densification. For example, HIP processing is expected to produce ACWF products with high waste loadings and low porosities. Of course, this would not simplify waste form production because HIP processing is more complicated than the PC method.

The dissolution behaviors of the ACWF products made with 11, 12, or 14 mass% ER salt loading are consistent with those of standard CWF products made with 8% EBR-II salt using P57 and Corning 7056 binder glasses. In ASTM C1308 tests conducted to study and compare the dissolution behaviors, all show an initial transient dissolution of NaCl from halite exposed at the surface followed by the slow dissolution of sodalite and glass phases. Degradation processes determined for CWF products occur for ACWF materials and predictive models developed for CWF products are applicable to ACWFs.

The conceptual model and understanding of the corrosion behavior based on extensive testing, analyses, and modeling of various CWF products made with P57 glass is relevant and applicable to ACWF materials and has benefited their development, especially the seminal work by Lambregts and Frank on CWF materials made with Cs-rich salts. Knowledge of the reactions that occur during waste form production can be used to formulate recipes that optimize immobilization of the waste salt and predict waste form performance.

The ACWF products made with 11% salt loading by using all five NBS glasses generated about twice as much sodalite as the material with 11% salt loading made using P57 glass. All ACWF products had higher initial Cl^- and Na releases (attributed to halite) that did CWF products made with 8% salt loading and also had small but measurable initial releases of Cs and other salt constituents, which indicates the waste salt was not completely sequestered in the glass phase. It is not certain if this is due to the formulation or processing conditions.

The NBS-4 binder glass composition was selected for use in ACWF materials being used to determine the maximum and optimum waste loadings and reduce the porosity. The ACWF made with NBS-4 glass had the highest sodalite content of the products made with 11% salt loading, had an acceptably low halite content based on XRD analysis, appeared to contain the smallest amount of residual unincorporated salt based on these dissolution tests, and had the lowest porosity based on measured water retention.

The NBS-4 glass composition provides sufficient Na to immobilize the Cl^- in waste salt as sodalite and optimize waste salt loading. There is no need to formulate another binder glass with a higher Na_2O content.

A 14% waste salt loading resulted in incomplete incorporation of Cs (which represents the waste salt contaminants) into the glass phase and the unreacted salt remained as accessible salt inclusions. This resulted in an increased initial release of Cs, but did not significantly decrease the waste form durability.

Essentially all the contaminants are contained in the glass phase at 12% salt loading, but the porosity of the ACWF is high due to the relative volumes of the sodalite and glass phases. Use of smaller zeolite 4A particles did not reduce the porosity. Using more glass will lower the waste loading in the final product

on a mass basis, but it is not expected to significantly increase the ACWF volume or salt loading in a disposal container.

It is expected that salt wastes with little or no Na^+ can be immobilized in ACWF materials made with NBS-4 binder glass, albeit at low waste loadings. These could include waste salts with higher contents of particular alkali metals, alkaline earths, or lanthanides than the ER salt compositions. The CWF-based waste forms remain the best option for immobilizing chloride waste salts.

The formulations of waste forms for HLW salt wastes must consider radiation and thermal limits that are based on the amount of waste salt in a disposal canister rather than achieving the maximum mass-based waste loading. These considerations will impact the benefits of optional fuel processing, separations, and waste treatment operations to the overall waste management strategy of the closed fuel cycle.

REFERENCES

ANS (2015). *Measurement of the Leachability of Solidified Low-level Radioactive Wastes by a Short-term Test Procedure*. American Nuclear Society standard ANSI/ANS-16.1, LaGrange, IL.

ASTM (2015a). *Standard Test Method for Accelerated Leach Test for Diffusive Releases from Solidified Waste and a Computer Program to Model Diffusive, Fractional Leaching from Cylindrical Waste Forms*. ASTM C1308-08. ASTM International Book of Standards Volume 12.01. West Conshohocken, PA.

ASTM (2015b). *Standard Test Method for Static Leaching of Monolithic Waste Forms for Disposal of Radioactive Waste*. ASTM C1220-10. ASTM International Book of Standards Volume 12.01. West Conshohocken, PA.

ASTM. (2015c). *Standard Test Methods for Determining Chemical Durability of Nuclear Waste Glasses: The Product Consistency Test (PCT) Standard C1285-08*, Annual Book of ASTM Standards Vol. 12.01, American Society for Testing and Materials, West Conshohocken, PA.

Bateman, K., Knight, C.J., and Solbrig, C.W. (2007). *Current Status of Ceramic Waste Form Development*. INL report INT/INT-06-11736.

Cheary, R.W., Coelho, A.A., and Cline J.P. (2004). *Fundamental Parameters Line Profile Fitting in Laboratory Diffractometers*. Journal of Research of the National Institute of Standards and Technology, 109 (1) 1-25.

Ebert, W.L. and Snyder, C.T. (2015). *Corrosion Tests with Waste Forms Developed for EChem Salt Wastes*. DOE NE report FCRD-MRWFD-2015-000145. Argonne National Laboratory.

Ebert, W. (2005). *Testing to Evaluate the Suitability of Waste Forms Developed for Electrometallurgically Treated Spent Sodium-Bonded Nuclear Fuel for Disposal in the Yucca Mountain Repository.* Argonne National Laboratory report ANL-05/43.

Ebert, W., Deitz, N., and Janney, D. (2005). *Effects of Heat-Treatment and Formulation on the Phase Composition and Chemical Durability of the EBR-II Ceramic Waste Form.* Argonne National Laboratory report ANL-05/32.

Ebert, W.L., Lewis, M.A., and Johnson, S.G. (2002). "The Precision of Product Consistency Tests Conducted with a Glass-Bonded Ceramic Waste Form." *Journal of Nuclear Materials* 305:37–51.
Federal Register (2000). *Record of Decision for the Treatment and Management of Sodium-Bonded Spent Nuclear Fuel.* Federal Register, Vol. 65, No. 182, pp. 56565–56570 (September 19, 2000).

Frank, S. (2014). Personal communication. May 15, 2014.

Frank, S. to T.P. O'Holleran (2004). "Product Consistency Test and Density Measurement Results from Surrogate CWF Inter-Granular Glass Material" ANL-W Memo ENT-MS-(SMF)-04-005, August 26, 2004.

Frank, S.M. (2002). "Alpha Decay Damage Study of a Glass-Bonded Sodalite Ceramic Waste Form." *Scientific Basis for Nuclear Waste Management XXV, Symposium held November 26–29, 2001.* Boston, Massachusetts. McGrail, B.P., and Cragnolino, G.A., eds. Vol. 713, pp. 487–494.

Stephane Gin, S., Patrick Jollivet, P., Fournier, M, Angeli, F., Frugier, P., and Charpentier, T. (2015) "Origin and consequences of silicate glass passivation by surfaces layers." *Nature Communications 6*, Article 6360.

Gombert, D., R. Counce, A. Cozzi, J. Crum, W. Ebert, C. Jantzen, J. Jerden, Jr., R. Jubin, M. Kaminski, V. Maio, J. Marra, T. Nenoff, R. Scheele, H. Smith, B. Spencer, D. Strachan, and J. Vienna. (2007). *Global Nuclear Energy Partnership Integrated Waste Management Strategy Waste Treatment Baseline Study Vol. I and Vol. II*. DOE report GNEP-WAST-AI-RT-2007-000324. Idaho National Laboratory.

Lacks, D.J., and Gordon, R.G. (1993). "Crystal-Structure Calculations with Distorted Ions." *Physical Review B, 48*, 2889-2908.

Lambregts, M.J., and Frank, S.M. (2003). "Characterization of Cesium Containing Glass-Bonded Ceramic Waste Forms." *Microporous and Mesoporous Materials, 64*, 1-9.

Lambregts, M.J., and Frank, S.M. (2002). "Preliminary Studies of the Disposition of Cesium in a Glass-Bonded Sodalite Waste Form." *Scientific Basis for Nuclear Waste Management XXV, Proceedings of the Materials Research Society Symposium held November 26–29, 2001.* Boston, Massachusetts. McGrail, B.P., and Cragnolino, G.A., eds. Vol. 713, pp. 373–380. Warrendale, Pennsylvania: Materials Research Society.

Lewis, M.A., Hash, M.C., Hebden, A.S., and Ebert, W.L. (2002). *Tests with Ceramic Waste Form Materials Made by Pressureless Consolidation*. Argonne National Laboratory Report ANL-02/10.

Li, H., Vienna, J.D., Hrma, P., Smith, D.E., and Schweiger, M.J. 1997. "Nepheline Precipitation in High-Level Waste Glass: Composition Effects and Impact on Waste Form Acceptability." *Scientific Basis for Nuclear Waste Management XX*, Materials Research Society Symposium Proceedings 465, pp. 261–268. Materials Research Society, Pittsburgh, PA.

McCloy, J.S., Riley, B.J., Lipton, A.S., Windisch, C.F.,Jr., Washton, N.M., Olszta, M.J., and Rodriguez, C.P. (2013). "Structure and chemistry in halide lead-tellurite glasses." *Journal of Physical Chemistry, 117*, 3456-3466.

Morss, L.R.; Mertz, C.J.; Kropf, A.J.; and Holly, J.L. (2002a). "Properties of Plutonium-Containing Colloids Released from Glass-Bonded Sodalite Nuclear Waste Form." *Scientific Basis for Nuclear Waste Management XXV, Proceedings of the Materials Research Society Symposium held November 26–29, 2001.* Boston, Massachusetts. McGrail, B.P., and Cragnolino, G.A., eds. Vol. 713, 421–427. Warrendale, Pennsylvania: Materials Research Society.

Morss, L.R.; Johnson, S.G.; Ebert, W.L.; DiSanto, T.; Frank, S.M.; Holly, J.L.; Kropf, A.J.; Mertz, C.J.; Noy, M.; O'Holleran, T.P.; Richmann, M.K.; Sinkler, W.; Tsai, Y.; and Warren, A.R. (2002b). *Corrosion Tests with Uranium- and Plutonium-Loaded Ceramic Waste Forms.* Argonne National Laboratory report ANL-02/09. Argonne, Illinois: Argonne National Laboratory.

O'Holleran, T.P. (1999). T.P. O'Holleran to S.G. Johnson, "Ceramic Waste Form Intergranular Glass Composition," ANL-W Memo ENT-NWM-(TPO)-99-010 (1999).

Richardson, J.W., Jr. (1997). "Salt-Occluded Zeolite Waste Forms: Crystal Structures and Transformability." *Scientific Basis for Nuclear Waste Management XXIII, Symposium, held December 2–6, 1996.* Boston, Massachusetts. Gray, W.J, and Triay, I.R., eds. Vol. 465, 395–400. Pittsburgh, Pennsylvania: Materials Research Society.

Riley, B.J., Kroll, J.O., Pierce, D.A., Canfield, N.L., Williams, B.D., Snyder, M.M.V., Ebert, W.L., and Frank, S.M. (2015). *Electrochemical Waste Forms Research: Critical Gap Activities for Fiscal Year 2015*. DOE NE report FCRD-JFCS-2015-000706. Pacific Northwest National Laboratory.

Riley, B.J., Rieck, B.T., McCloy, J.S., Crum, J.V., Sundaram, S.K., and Vienna, J.D. (2012). "Tellurite glass as a waste form for mixed alkali-chloride waste streams: Candidate materials selection and initial testing." *Journal of Nuclear Materials, 424*, 29-37.

Riley, B.J., Kroll, J.O., Pierce, D.A., Canfield, N.L., Williams, B.D., Snyder, M.M.V., Ebert, W.L., and Frank, S.M. (2015). *Electrochemical Waste Forms Research: Critical Gap Activities for Fiscal Year 2015*. DOE report FCRD-JFCS-2015-000706.

Simpson, M.F. (2003). "Two-Site Equilibrium Model for Ion Exchange Between Monovalent Cations and Zeolite-A in a Molten Salt." *Industrial Engineering and Chemical Research*, 38, 2469–2473.

Simpson, M.F., and Battisti, T.J. (1999). "Adsorption of Eutectic LiCl-KCl into Zeolite 4A Using a Mechanically Fluidized Vacuum System." Ind. Eng. Chem. Res. 38:2469–2473.

Strachan, D.M. and Badad, H. (1979). "Iodide and Iodate Sodalites for the Long-Term Storage of Iodine-129," Rockwell International Report RHO-SA-83.

Stratton, S.W. (1924). Standard Density and Volumetric Tables, 6th ed. Washington: Government Printing Office.

Vance, E.R., Roy, R., Pepin, J.G., and Agrawal, D.K. (1982). "Chemical Mitigation of the Transmutation Problem in Crystalline Nuclear Waste Radiophases." *Journal of Materials Science, 17*, 947-952.

Vienna, J.D. (2015). Personal communication. February 17, 2015.

APPENDIX A

TECHNICAL DETAILS OF MATERIAL PRODUCTION AND ANALYSES

APPENDIX A

Technical Details of Material Production and Analysis

A.1 Salt simulant preparation

The salt simulant was made starting with high (≥99.99%) purity, anhydrous salts from Sigma Aldrich (St. Louis, MO) or Alfa Aesar (Haverhill, MA). All salt components were mechanically mixed in large polyethylene container and then poured into one of two alumina crucibles (4.6×15.2 cm). The crucibles were placed into a furnace (Applied Test Systems, Butler, PA) and heated to 550 °C for ~1 h. The molten salt was then poured from the crucible to a stainless steel tray and cooled. The salt was collected and ground to a powder by using a laboratory grinder (Mazzer, Venezia, Italy) and remixed. The salt was melted a second time, collected, ground to a powder, and mechanically mixed.

A.2 Zeolite 4A Preparation

Zeolite 4A was purchased (UOP, Des Plaines, IL) in the form of 0.5-mm spherical aggregates with ~4 mass% clay binder and was ground by using a roller mill and sieved to isolate the 45–250 µm size fraction (Gilson Company, Lewis Center, OH). The sized zeolite 4A powder was then dried by placing it into a ~2 L vacuum-tight steel vessel. The drying vessel was placed into a vertically-oriented cylindrical furnace and heated under a continuous flow of argon gas (approximately 0.2 L min^{-1}). The vessel was heated at a ramp rate of ~10 °C min^{-1} to ~150 °C and held for several hours so that the large amount (~22 mass%) of water vapor could be released from the zeolite 4A. The temperature was then increased to 500 °C and held at that temperature for 28 h under a continuous flow argon gas then allowed to cool. After the vessel had cooled to room temperature, the inlet and outlet line valves were closed and the vessel was transferred to an argon atmosphere glove box where the powder was remove from the vessel. All subsequent zeolite powder handling was performed under an inert atmosphere to prevent rehydration of the zeolite 4A.

The moisture content of the zeolite 4A after drying was determined by Karl Fischer titration. The titrator (Mitsubishi CA-200, Chesapeake, VA, USA) was connected to a high temperature furnace where a sample of the powdered sample was introduced. Water that evolved from the sample as it was heated was swept by flowing inert gas into the reaction/titration vessel in which the moisture content was quantitatively determined. The average moisture content based on the analyses of several samples of dried zeolite 4A was determined to be 0.24 ± 0.06 mass%.

A.3 Salt Occlusion

Salt occlusion into the zeolite 4A was performed by hand-mixing the targeted amounts of sized salt and dried zeolite powder in a sapphire mortar and pestle. Two batches of SLZ were prepared for CWF fabrication with each mixture containing approximately 11.4 g of salt and 65.1 g of zeolite 4A. Following hand mixing, the powder was placed into a 200 mL glass carbon crucible and placed in a 500 °C furnace. After about 2 h, the mixture was removed from the furnace and stirred for several minutes, then placed back into the furnace for another 2 h. This process was repeated three additional times. The mixture was left in the furnace for 12 h after the final stirring and then mixed one last time before cooling to ambient temperature.

A so-called "free Cl^- analysis" was performed to measure the degree of salt occlusion for each batch of SLZ. In this analysis, a 0.5-g sample of SLZ is placed in 30 mL of demineralized water and shaken

vigorously for 1 minute. The solution is then immediately passed through a 0.45-µm pore-size filter. The Cl^- concentration in the collected water fraction is measured with an ion-selective electrode (Orion 290A meter, Thermo Scientific, Waltham, MA, USA). Free Cl^- analyses were performed on several samples of each batch and the overall average free Cl^- concentration was 0.15 ± 0.01 mass% Cl^-. This is well below the threshold of 0.5 mass% used for EBR-II waste forms (Ebert 2005).

A.4 Binder Glasses

When P57 glass was melted, casted, and annealed for making bars for dilatometry measurements, the resulting glass contained lots of tiny bubbles. Since these bubbles interfere with the thermal expansion during dilatometry measurements, the P57 glass was remelted with 0.5 mass% Na_2SO_4 added as a fining agent to remove bubbles and create a fully dense glass bar. This provided bars that were bubble-free for dilatometry samples. The glasses poured at a very high viscosity, even at the high melting temperatures (T_M = 1450-1550 °C). The T_g and T_s values measured for P57 with added Na_2SO_4 were 516 °C and 507 °C, respectively, which are very close to the values of 570 °C and 567 °C, respectively, that were reported by O'Holleran (1999). However, the T_g and T_s values measured for all of the NBS glasses were higher than those for P57 glass: ΔT_g = 36–54 °C and ΔT_s = 15–38 °C. The values for NBS-4 glass were closest to P57 glass (ΔT_g = 36 °C and ΔT_s = 15 °C). Nevertheless, all NBS glasses met the criteria that had been used by Bateman et al. (2007) to ensure that the glass softening temperature was <750 °C.

A.5 CWF and ACWF Product Fabrication

To fabricate each CWF and ACWF product, a 50-g mixture comprised of the appropriate masses of SLZ and glass were mixed in a mortar and pestle then poured into a 200-mL glassy carbon crucible. The loaded crucibles were heated to 925 °C and held for 16-20 h then allowed to cool slowly by turning the power to the furnace off.

A.6 Archimedes measurements of porosity and density

The mass of each dry specimen (m_{dry}) was measured by using an XPE20 analytical balance (Mettler Toledo). The specimen was then submerged in absolute ethanol within a vacuum desiccator to remove air from the open porosity and back-fill the voids with absolute ethanol. After submersion under vacuum (1.3–6.7 Pa) for about 20 minutes, the submerged mass (m_{sub}) was measured using an Archimedes apparatus. The pellet was then removed from the ethanol and excess ethanol on the surface was removed by blotting with an ethanol-soaked cloth. The pellet with the pores filled with ethanol was weighed (m_{sat}). The temperature of the ethanol was monitored and used to calculate the bulk Archimedes density (ρ_a) of the pellet according to Equation A.1 where the ρ_{EtOH} was the density of ethanol (from Stratton 1924: $\rho_{EtOH} = -8.54\times10^{-4}\ T + 0.806$; for T = 15–25 °C). From these data, the open porosity (ϕ) of the specimens was calculated based on mass differences (ϕ_m) by using Equation A.2 (Lacks and Gordon 1993)

$$\rho_a = (m_{dry} \times \rho_{EtOH}) / (m_{sat} - m_{sub}) \quad (A.1)$$

$$\phi = (m_{sat} - m_{dry}) / (m_{sat} - m_{sub}) \quad (A.2)$$

A.7 Scanning Electron Microscopy and Energy Dispersive Spectroscopy

Pieces of each CWF and ACWF material were vacuum-impregnated with resin and polished in glycol-based diamond suspensions to a 1-µm finish. Polished cross-sections were examined by using a scanning electron microscope (SEM) with a backscattered electron (BSE) detector for atomic number contrast. Analyses at ANL were conducted using a Hitachi S-4700-II SEM and analyses at PNNL were conducted using a JSM-7001F field-emission gun microscope (JEOL USA, Inc. Peabody, MA). Samples were first

carbon-coated (ANL) or sputter-coated with platinum (PNNL; Polaron Range SC7640, Quorum Technologies Ltd., East Sussex, England). Energy dispersive x-ray emission spectroscopy (EDS) was performed with a Bruker xFlash® 6|60 (Bruker AXS Inc., Madison, WI). The EDS dot mapping was performed at 110–130 k counts s^{-1} with a ~51-min collection time over 1024×768 pixels at a 16-µs dwell time per pixel. Line scans were performed on the collected maps using 512 vertical data points that were averaged along the horizontal data collection line.

A.8 Time-of-flight secondary ion mass spectrometry

A time-of-flight-secondary ion mass spectrometer (ToF-SIMS; TOF.SIMS5, IONTOF GmbH, Münster, Germany) was used to perform elemental mapping with a lateral resolution of ~ 200 nm. A thin layer of Au (~10 nm) was deposited on the specimen surface to minimize charging effects. To remove the Au layer for analysis and remove possible surface contamination, a 1.0 keV O^{2+} beam was used as a sputter beam, which was scanned on a 200×200-µm area until a stable signal was obtained. Analysis was performed by scanning a 25.0 keV Bi^{+} beam at a current of 0.273 nA on a 20-µm × 20-µm area around the center of the O^{2+} crater. The secondary ion images were taken after the surface had been cleaned with the O^{2+} beam. All analyses were made with 256×256 pixels per image.

A.9 X-ray Diffraction

A section from each CWF and ACWF material was analyzed with a Bruker D8 Advance XRD with Cu K_{α} emission and a LynxEye™ position-sensitive detector with a collection window of 3° 2θ. Scan parameters were 5–75° 2θ with a step of 0.015° 2θ and a 0.6-s dwell at each step. About 5 mass% NIST SRM-674b (TiO_2) was added to each of the powdered materials to quantify the amorphous fractions. Bruker AXS© EVA (v14) and Topas (v4.2) software were used to identify and quantify phase assemblages. Rietveld refinements were performed using whole-pattern fitting following the fundamental parameters approach (Cheary et al. 2004).